



University
of Glasgow

<https://theses.gla.ac.uk/>

Theses Digitisation:

<https://www.gla.ac.uk/myglasgow/research/enlighten/theses/digitisation/>

This is a digitised version of the original print thesis.

Copyright and moral rights for this work are retained by the author

A copy can be downloaded for personal non-commercial research or study, without prior permission or charge

This work cannot be reproduced or quoted extensively from without first obtaining permission in writing from the author

The content must not be changed in any way or sold commercially in any format or medium without the formal permission of the author

When referring to this work, full bibliographic details including the author, title, awarding institution and date of the thesis must be given

Enlighten: Theses

<https://theses.gla.ac.uk/>
research-enlighten@glasgow.ac.uk

A STUDY OF SOME NEUTRON INDUCED REACTIONS

by

W.T. MORTON

Department of Natural Philosophy

University of Glasgow

Presented as a thesis for the degree of Ph.D.

in the University of Glasgow,

September 1958.

ProQuest Number: 10656215

All rights reserved

INFORMATION TO ALL USERS

The quality of this reproduction is dependent upon the quality of the copy submitted.

In the unlikely event that the author did not send a complete manuscript and there are missing pages, these will be noted. Also, if material had to be removed, a note will indicate the deletion.



ProQuest 10656215

Published by ProQuest LLC (2017). Copyright of the Dissertation is held by the Author.

All rights reserved.

This work is protected against unauthorized copying under Title 17, United States Code
Microform Edition © ProQuest LLC.

ProQuest LLC.
789 East Eisenhower Parkway
P.O. Box 1346
Ann Arbor, MI 48106 – 1346

CONTENTS

<u>PREFACE</u>		Page
<u>CHAPTER I</u>	<u>INTRODUCTION</u>	
(i)	Introduction	1.
(ii)	Compound Nucleus and Statistical Models	3.
(iii)	Experiments Testing Validity of Statistical Assumption	9.
(iv)	Independent Particle Model	16.
<u>CHAPTER II</u>	<u>(n,α) REACTIONS IN COMPLEX NUCLEI</u>	
(i)	Introduction	24.
(ii)	(n, α) Reactions In Emulsion Nuclei	25.
(iii)	Exposure and Development of Emulsions	28.
(iv)	Calculation of the Cross Section.	32.
(v)	Further (n, α) Studies by Other Workers	33.
<u>CHAPTER III</u>	<u>(n,p) REACTIONS IN NATURAL ALUMINIUM AND RHODIUM</u>	
(i)	Introduction	35.
(ii)	Apparatus	35.
(iii)	Examination of Emulsions	37.
(iv)	Analysis	38.
(v)	Discussion of Aluminium and Rhodium Results	42.

CHAPTER IV (n,p) REACTIONS IN Fe⁵⁴, Fe⁵⁶ and Ni⁶⁰

(i)	Introduction	50.
(ii)	Apparatus, Exposure and Development of Emulsions	52.
(iii)	Examination of Emulsions	56.
(iv)	Analysis of Tracks	59.
(v)	Analysis of Results	61.
(vi)	Angular and Energy Distributions	63.
(vii)	Nuclear Temperatures	68.
(viii)	Comparison of Results with Other Workers	71.
(ix)	Comparison With Direct Interaction Theories	73.
(x)	A Modification To The Theory of Brown and Muirhead	75.

CHAPTER V COLLIMATED NEUTRON BEAM STUDY OF ALUMINIUM

(i)	Introduction	78.
(ii)	Apparatus and Exposure	80.
(iii)	Neutron Flux and Efficiency of Collimator	84.
(iv)	Scanning Procedure and Analysis of Data	86.
(v)	Energy and Angular Distributions	88.

CHAPTER VI 960 MeV NEUTRON INDUCED REACTIONS

(i)	Introduction	94.
(ii)	Neutron Source and Exposure Conditions	96.
A. <u>Complex Nuclei Events</u>		
(i)	Scanning Procedure	97.
(ii)	Analysis of Events	98.
(iii)	Division of Events into Heavy and Light Nuclei	99.
(iv)	Prong Distribution	103.
(v)	Energy Distribution of Prongs	106.
(vi)	Angular Distribution of Prongs	108.
B. <u>n-p Interactions</u>		
(i)	Analysis of Events	109.
(ii)	Cross Section for $n+p \rightarrow p+p+\pi^-$	111.
Future Prospects.		

PREFACE

During the past three years the author has undertaken the study of some nuclear interactions induced by neutrons, using nuclear research emulsions to detect the products of the reaction.

At the outset of this work, the mechanism of neutron induced reactions at an energy ~ 14 MeV was not clear. The possibilities were either that the reaction proceeded through the formation of a compound nucleus, or by means of a direct interaction, or a combination of both.

Neutron activation experiments of Paul and Clarke had suggested the occurrence of a large direct interaction in both (n,p) and (n,α) reactions at this energy for a large number of different nuclei. Since such direct (n,α) reactions appear unlikely as they would involve alpha particle subgroups in all nuclei, this process was investigated first. Nuclear research emulsions were irradiated with neutrons with an energy ~ 14 MeV and the emulsions searched for evidence of an alpha particle and electron starting at the same point, indicating an (n,α) reaction in Ag or Br. The observed cross section for this process was much smaller than the previously reported value. Later work performed by a number

of authors, although not performed for the same elements, has shown cross sections similar to those obtained by the present author for the Ag and Br study. This work, described in Chapter II, was undertaken entirely by the author.

Chapter III describes a joint investigation with G.Brown of the angular and energy distribution of protons emitted from Al and Rh foils on bombardment with uncollimated neutrons with an energy ~ 14 MeV. The author performed the volume scanning necessary for the analysis of the results and shared equally in the analysis. The results of this experiment strongly suggested the occurrence of direct interaction.

The remainder of the work described in subsequent chapters of this thesis was performed independently by the author under the supervision and guidance of Dr. P.V.March.

To elucidate further the nature of direct interaction a series of experiments, described in Chapter IV, were performed on proton emission, under neutron bombardment, from the separated isotopes Fe^{54} , Fe^{56} and Ni^{60} . These results provided more information upon both the direct interaction mechanism and upon the decay of the compound nucleus. The results were compared with theories of direct interaction, and a modification by the author to existing theories is described. This modification in

which angular momentum conservation is assumed gives angular distributions in good agreement with experiment.

The work previously described suffered from the disadvantage of a large background subtraction due to protons starting within the emulsion but unresolvable from protons starting outside. By the use of higher neutron fluxes and a neutron collimator, as described in Chapter IV, a detailed energy spectrum was obtained from aluminium. The energy spectra of deuterons and protons at forward and backward angles were found to exhibit structure. The energy levels observed are shown to be in good agreement with those observed by other workers in reactions leading to the same residual nuclei.

The cross section for the reaction $n+p \rightarrow p+p+\pi^-$ at high energies is of particular importance because of its dependence on the concept of charge independence. Previous experiments performed on this reaction and other reactions are in disagreement concerning the cross section for the reaction $n+p \rightarrow p+p+\pi^-$ at energies ~ 900 MeV. Nuclear research emulsions were exposed to the 900 MeV neutron beam from the Birmingham synchrotron by B. Munir and the emulsions analysed, as described in Chapter V, by the author for $n+p \rightarrow p+p+\pi^-$ events. A cross section was obtained in

agreement with the previous measurement of the cross section for this reaction.

The neutron flux was monitored by means of the interaction of neutrons with the complex nuclei of the emulsion. The characteristics of these disintegrations are given. No previous studies of neutron interactions with the complex nuclei of nuclear research emulsions have been at sufficiently high energy for meson production to play an important part.

W. T. Morton

CHAPTER I

INTRODUCTION

(i) Introduction

The central problem of nuclear physics is the description of the forces acting between nucleons. Studies of the interactions of nucleons with nuclei soon showed that known forces could not be used to explain nucleon-nucleon interactions and a new type of force - the nuclear force - was postulated. No complete description of the interaction between two free nucleons exists at present. Apart from this difficulty there is no experimental evidence that the interaction of two nucleons within nuclei are similar, except for the restrictions of the Pauli principle, to free nucleon-nucleon interactions. Doubt is also present (e.g. Weisskopf, 1957) concerning the mass of a nucleon within complex nuclei. Thus at the present time any attempt to explain nuclear reactions must proceed by means of apparently plausible assumptions often guided by classical considerations. The particular choice of assumptions may be taken as the definition of a nuclear model.

Many nuclear models are in vogue at the present time, each with its strictly limited range of validity. In general these models can be classified into two groups according as to whether a nuclear reaction is assumed to involve all the nucleons of the nucleus or only a few of the nucleons. In the compound nucleus model, in which all the nucleons of the nucleus partake in the reaction, it might at first be supposed that the nucleon-nucleus interaction is strong. In the independent particle model, in which nucleons are supposed to move freely, and can be assigned definite quantum states, it might be supposed that the nucleon-nucleus interaction is weak. Within the last few years it has been realised that this apparent contradiction can be explained.

The first part of this thesis concerns experiments in the energy region where the compound nucleus model appears to breakdown. Experimental results have been obtained which cannot wholly be explained by the compound nucleus model. A modification will be proposed to a theory which considers nuclei as having both compound nucleus and independent particle properties, and this theory will be compared to the experimental results.

(ii) Compound Nucleus and Statistical Models

Experiments performed by Moon and Tillman (1935) and Fermi and Amaldi (1935) and by others indicated large fluctuations in the cross section for slow neutron scattering for small energy variations. The large number of closely spaced resonances suggested a many particle problem.

To explain the closely spaced resonances found experimentally at low bombarding energies the compound nucleus model was advanced by Bohr (1936). This model may be referred to as the 'Bohr compound nucleus model' to distinguish it from a model discussed later. Bohr proposed that nuclear reactions should be considered as divided into two stages. In the first stage the projectile amalgamates with the bombarded nucleus to form a compound state, in which the energy of the projectile is shared with the nucleons of the bombarded nucleus within a very short time of the order of 10^{-21} seconds. That is a time corresponding to the time the projectile would take to pass over a distance equal to the diameter of the nucleus. Intuitively Bohr argued that after a long time (much greater than 10^{-21} seconds) enough energy might be concentrated on a single particle or group of particles

to allow it to escape. Hence in the Bohr compound nucleus model the decay of the compound system bears little relation to the manner in which it was formed.

The basic predictions of Bohr's compound nucleus model are that the emitted particles should have an isotropic angular distribution and that the energy spectra should have the Maxwellian shape common to all evaporation processes. The energy spectra for charged particles will be modified by the Coulomb barrier. Through all stages of the reaction it is of course necessary that total energy, angular momentum and parity must be conserved.

The lack of correlation between formation and decay can be expressed mathematically by writing the cross section for a particular reaction as the product of two quantities. The first term represents the cross section for the formation of a compound system, or sticking probability. The second term represents the probability for the decay of the compound system by a particular mode. Hence the second term is given as the ratio of the probability for the decay by one mode to the sum of the probabilities of decay by all modes. Let the reaction



be considered, where a is the incident particle, b is

the emitted particle and A and B are the initial and final nuclei respectively. Let $\sigma_c(a)$ be the cross section for the formation of a compound nucleus by a particle a at the excitation considered. Let τ_b be the mean life of the compound system for the decay by means of particle b. Then the cross section for the process (a,b) is

$$\sigma(a,b) = \sigma_c(a) \frac{\frac{1}{\tau_b}}{\sum_i \frac{1}{\tau_i}} \quad (2)$$

It is usual to define Γ as $\Gamma = \frac{h}{\tau}$ and so the units of Γ are those of energy. Because of its part in resonance reactions it is usual to refer to Γ as a width. Equation (2) now takes the form

$$\sigma(a,b) = \sigma_c(a) \frac{\Gamma_b}{\sum_i \Gamma_i} \quad (3)$$

By applying the principle of detailed balancing the cross section for a particular mode of decay is expressed in terms of the cross section for the formation of a compound nucleus by the type of particle whose emission spectrum is required (Weisskopf 1937, Weisskopf and Ewing 1940). The final expression for the number of particles N_i of type i and with energy between E and E+dE emitted by a compound nucleus is obtained as

$$N_i(E) dE = K \sigma_{ci}(E) E \omega dE \quad (4)$$

where/

where $\sigma_{ci}(E)$ is the cross section for the formation of a compound nucleus by a particle of type i and with energy $E = E - Q$ (where Q is the Q -value of the reaction), ω is the level density of the residual nucleus and K is a constant.

The constant K is determined by the various possible modes of decay. It is usual to assume that the emission of protons, neutrons, deuterons and alpha particles can be treated on an equal footing.

The variation of the level density is not known with accuracy from nucleus to nucleus. The best level density formula only predicts level densities to within a factor of 3 (Newton 1956, Cameron 1957).

In order to calculate the cross section for the formation of a compound nucleus it is necessary to make further assumptions. It is well known that for light nuclei the energy dependence of the total cross section is accurately given by nuclear dispersion theory. Bethe (1940) and Feshbach, ~~Emmer~~ and Weisskopf (19⁴⁹~~54~~) developed a method to obtain the variation of the cross section with bombarding energy for heavy nuclei. This simplified quantum mechanical calculation is usually referred to as the

continuum theory. In this theory the range of nuclear forces is assumed to be well defined. A particle which penetrates into the nucleus is assumed to have an energy given by the sum of its energy outside and the kinetic energy of internuclear motion. No individual properties of nuclei such as resonances are considered. The only parameters required are the nuclear radius and the wave number of the projectile within the nucleus. This theory predicts that the cross section for neutron induced reactions is a smooth function of mass number and that the total cross section is a monotonic decreasing function of neutron energy.

Cross sections for the formation of the compound nucleus by charged particles have been calculated by Shapiro (1953). Here the projectiles are regarded as individual particles and so this theory does not include deuteron stripping. These calculations which depend essentially on the barrier penetrability appear to be in agreement with the (p,n) experiments of Blaser et al. (1951 a and b). The cross section for the formation of the compound nucleus by a particle of de Broglie wavelength λ and angular momentum l has the form

$$\sigma_c^l = \pi \lambda^2 (2l+1) T_l \quad (5)$$

where T_e is the Coulomb penetrability factor. It would be expected that only particles with $l < \frac{R}{\lambda}$ would interact strongly with the nucleus where R is the nuclear radius. If T_e is assumed to be unity and summation in equation (5) is carried out from $l=0$ to $l = \frac{R}{\lambda}$ then the cross section is found to equal $2\pi R^2$, or twice the geometrical cross section.

Quantum mechanically the resonance phenomena are observed in slow neutron scattering ~~is~~ described by quasi stationary eigenstates of the compound system. The second stage of the Bohr compound nucleus model must be represented as a sum over eigenstates. Hence the second stage is only valid when the sum over eigenstates is valid, that is at sufficiently high energy or when the beam of bombarding particles is sufficiently non-monoenergetic.

The work of Kapur and Peierls (1938) and Wigner and Eisenbud (1947) has shown how the idea of resonance eigenstates can be enlarged to define a complete mathematical description of nuclear reactions. This approach is now often referred to as the compound nucleus model e.g. Peaslee (1955). Using this definition the compound nucleus model must always be valid for nuclear

reactions. Unfortunately this method of approach does not produce new physical information concerning the nucleus.

A simplification of the compound nucleus (eigenstate) problem is the statistical assumption. Here there is assumed to be no correlation between neighbouring eigenstates. It is this statistical model which has the properties proposed by Bohr; that is a lack of correlation between the modes of decay and formation.

Using the statistical assumption it is possible to obtain, under general conditions (Wolfenstein, 1951), the angular distribution of the emitted particles as a function of $\cos^2\theta$, where θ is the angle between the incoming and outgoing particles, in a nuclear reaction. Hence the angular distribution of the emitted particles is symmetric about 90° on the basis of the statistical assumption. Any departure from this symmetry will indicate the failure of the statistical assumption.

(iii) Experiments Testing Validity of Statistical Assumption

As more accurate experiments become available it is important to test the fundamental assumptions

on which the statistical model is based. These assumptions are that a compound system is formed immediately by the bombarding particle and that the mode of decay of the compound system is independent of the mode of formation (independence hypothesis).

The independence hypothesis is difficult to test experimentally. To test this hypothesis it is necessary to form a compound system containing the same number of neutrons and protons at the same excitation energy by bombarding different nuclei. The validity of this hypothesis would be expected to depend on the nuclei and excitation energy involved.

The reaction $N^{14}(n,p)C^{14}$ has been studied by Stebler and Huber (1948) and the reaction $C^{14}(p,n)N^{14}$ by Shoupp et al. (1949). These reactions both involve the compound nucleus N^{15} and the same levels were found in this compound nucleus in both reactions. This result, by itself, since it is obtained by a mirror reaction, only indicates the validity of the reciprocity theorem and does not give information on the independence hypothesis. However, the compound nucleus N^{15} is also formed in the reactions $N^{14}(n,\alpha)B^{11}$ and $B^{11}(\alpha,n)N^{14}$ which were studied by Stebler and Huber (1948) and Walker (1949) respectively,

and the same energy levels observed. The validity of the statistical assumption is indicated by the two sets of experiments having resonances at the same energy values within the experimental errors. These experiments indicate the validity of the independence hypothesis in the region of a few MeV excitation energy for light nuclei.

An experiment performed by Goshal (1950) seems to give evidence in favour of the independence hypothesis for excitation energies in the energy region of 15-40 MeV and middle weight nuclei. By suitably adjusting the energy of the bombarding particle, to take into account differences in binding energy, the compound system Zn^{64} was obtained with the same excitation energy by bombarding Ni^{60} with alpha particles and Cu^{63} with protons. The decay of this system by means of a neutron, two neutrons and a proton and a neutron was investigated. The ratios of the cross sections of these processes formed by the two different methods were found to agree suggesting the validity of the independence hypothesis. However, a discrepancy exists between the Q values suggested by this experiment and the Q values obtained from mass measurements. Subsequent mass

measurements (Eastman et al. 1956) confirm this discrepancy.

The validity of the independence hypothesis with regard to heavy elements was investigated by John (1956). In this experiment the excitation function of the reaction $\text{Pb}^{206}(\alpha, xn)$ was investigated where $x=2,3,4$. He compared the results of his experiments with the results of Kelly (1950) who studied the reaction $\text{Bi}^{209}(p, xn)$, again, where $x=2,3,4$. The same compound nucleus participates in both reactions. If the independence hypothesis is valid it should be possible to shift the energy scale of the excitation curves so that

$$\sigma(p, 2n) : \sigma(p, 3n) : \sigma(p, 4n) = \sigma(\alpha, 2n) : \sigma(\alpha, 3n) : \sigma(\alpha, 4n)$$

The shift in scale should be such that the same excitation of the compound nucleus is involved in both reactions. Although it is possible for the scale to be shifted to bring the cross sections into agreement there is again a small discrepancy between the magnitude of the Q values and the energy shift.

Experiments performed by Cohen and Newman (1955) were designed to investigate the relative probabilities of proton and neutron emission from nuclei in the same mass region, 48-71, when bombarded by protons with an energy of 21 MeV and neutrons with an energy of 14 MeV.

These experiments indicate that proton emission is more probable than neutron emission when the bombarding particle is a proton. This result is at variance with the independence hypothesis. It is not possible to bring these experiments into agreement by lowering the Coulomb barrier due to oscillations of the compound nucleus nor by adjusting the energy level formula at low excitation.

Experiments performed by Gugelot (1954) and Eisberg and Igo (1954) on inelastic proton scattering at energies of 18 MeV and 31 MeV, respectively, and by others, from various middle weight and heavy nuclei also do not agree with statistical model predictions. Energy spectra of protons were obtained with many more high energy particles than could be accounted for by an evaporation process. An asymmetry in the angular distribution about 90° was also found. More protons were found to be emitted in the forward direction: a result suggesting the occurrence of direct interaction.

Less sensitive than the study of angular distributions, and to a lesser extent energy spectra, were a number of experiments designed to measure total cross sections for particular reactions. The uncertainties

in these experiments are mainly in the values used for the penetrability of the Coulomb barrier. Nevertheless, Waffler (1950) using neutrons with an energy of 9 MeV and later Paul and Clarke (1953) using neutrons with an energy of 14 MeV obtained cross sections for neutron induced reactions much larger than predicted by the statistical model.

A critical analysis of the statistical model immediately shows that a breakdown is not wholly unexpected. It is necessary to consider the variation of the level width Γ and the level spacing D . When the level width is much less than the level spacing the reaction will show well separated resonances. This in general will occur for light nuclei. When the level width is much greater than the level spacing no individual levels may be distinguished and the phase differences from different levels might cancel. However, whether or not, in the region of overlap of resonances the differences in phase between individual levels do cancel has to be made the subject of experiment.

Because of the unsatisfactory nature of the statistical model in explaining some experiments it is necessary to examine in more detail the experiments

which give apparently anomalous results in the hope that they might give some indication of a more general model.

One of the main experiments to throw doubt on the absolute validity of the statistical model also gave an indication of a method of overcoming this difficulty. Experiments were performed by Miller et al. (1952) to clarify the variation of the total neutron cross section with mass number in the energy range from 0.1 to 3 MeV. These experiments showed, disregarding the effect of individual resonances, that neighbouring nuclei exhibit very similar variations of cross section with energy while elements far apart display appreciable differences. Barschall (1952) showed these results on a three dimensional plot. The axes represent energy, mass number and total cross section divided by the geometrical cross section. Further confirmation of these results have been obtained by Walt et al. (1953) and others. Part of these remarkable results is shown in figure 1.

The gradual change in cross section with mass number and energy suggests a simple picture of the nucleus such as a representation in terms of a potential well.

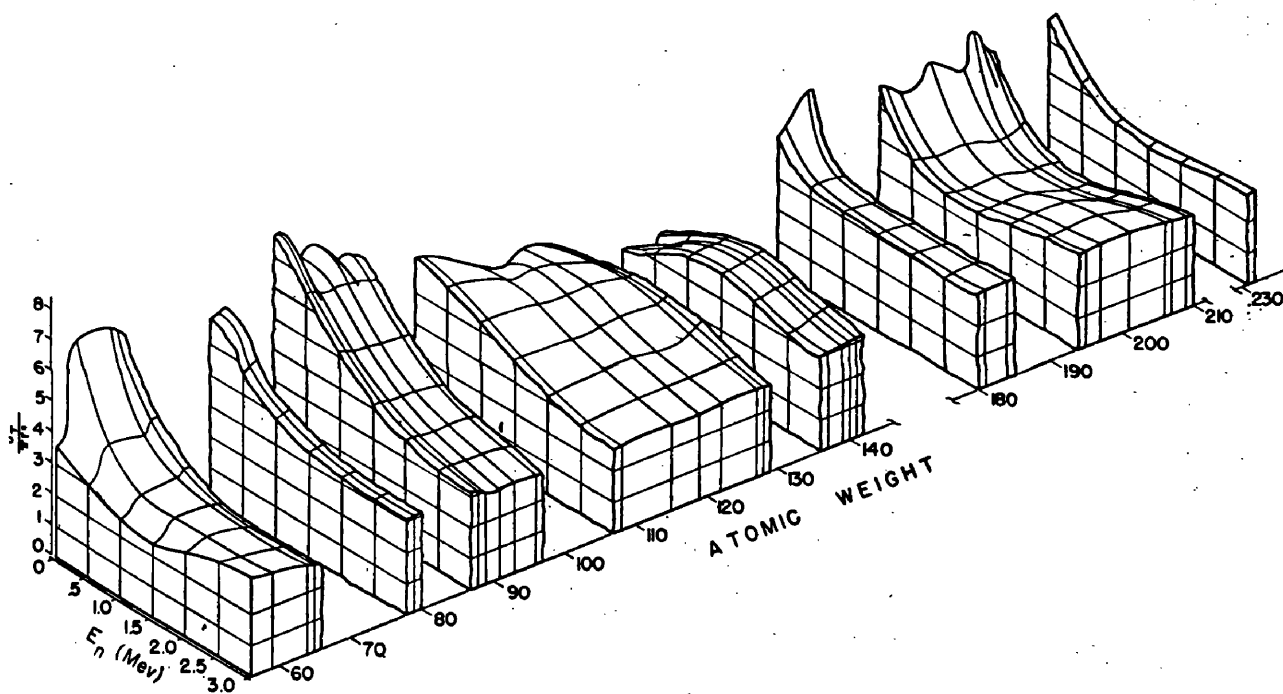


FIG. 1. Total neutron cross sections of elements heavier than Mn as a function of neutron energy. The surface is based on measurements for the atomic weights at which straight vertical lines appear in the figure.

(iv) Independent Particle Model

The first attempts to explain nuclear reactions supposed that the interaction of the projectile with the target nucleus could be approximated by a real potential well. The radius of the well was assumed to be comparable to the nuclear radius while the depth was considered to be a few MeV. According to this model the elastic scattering cross section was found to approximately equal the nuclear dimensions, while resonances are also predicted with an energy of 10 to 20 MeV apart. The closely spaced resonances found by Moon and Tillman (loc. cit.) and others led to the temporary abandoning of this model.

On the basis of the compound nucleus model it would be expected that the total cross section for neutron interactions at an energy of 90 MeV would be little different from the cross section at an energy of 14 MeV. The difference would be caused by the slightly different nuclear radius due to the difference in the de Broglie wavelength of the projectile. The neutron cross section at an energy of 14 MeV was measured by Amaldi et al. (1946). Experiments performed by Cook et al. (1949) on the

total cross section of 15 elements ranging from hydrogen to uranium for neutrons with an energy of 90 MeV gave cross sections considerably different from those obtained at an energy of 14 MeV. It was found that the cross section for light nuclei was appreciably lower than expected while the cross section for the heavier nuclei tended to the expected value.

Serber (1947) pointed out that at energies of the order of 100 MeV the ~~scattering cross section~~ ^{mean free path} of a neutron or a proton ~~with another nucleon~~ ^{in nuclear matter} will be of the order of the nuclear radius and consequently the nucleus will appear partially transparent to the bombarding particle. Fernbach, Serber and Taylor (1949) showed that the results of Cook et al. could be explained using a nuclear radius of $1.37 A^{1/3} \times 10^{-13}$ cm, a neutron energy within the nucleus of 31 MeV and a mean free path of a nucleon in nuclear matter of the order of 4.5×10^{-13} cm. The method of Fernbach, Serber and Taylor is known as the optical model. In the optical model the scattering of the incident particle is considered in an analogous manner to the scattering of light by a glass sphere. In both problems reflection, refraction and diffraction occur. The inelastic cross section is

obtained by considering the mean free path of nucleons in nuclear matter.

In order that the optical model will give the reaction cross section it is necessary to consider complex potential wells. The model in which the potential well has both real and imaginary parts is often referred to as the 'cloudy crystal ball model'. The simplest complex potential is

$$\begin{aligned} V &= -V_0(1+iS) \text{ for } r < R \\ V &= 0 \text{ for } r > R \end{aligned}$$

where r is the distance between the centre of the particle and the centre of the nucleus, R is the nuclear radius, V and S are constants depending on the energy of the bombarding particle. A model in which $S=1$ was employed by Bethe (1940) while Fernbach, Serber and Taylor (loc. cit.) used essentially this model. Ford and Bohm (1950) also used this model with $S=0$ while discussing zero energy scattering. In a proper treatment of the optical model it is essential to take into account the spin orbit interaction.

Feshbach, Porter and Weisskopf (1954) applied the optical model at low energies. They found that with a well depth of 42 MeV, $S=0.03$ and a nuclear radius

of $1.45 \text{ A}^{1/3} \times 10^{-13} \text{ cm}$ that the observed total neutron cross section could be reproduced. They also obtained good agreement with the neutron scattering cross section. Although showing qualitative similarity the ratio of neutron width to level spacing was not in good agreement.

Later Woods and Saxon (1954) found a well shape

$$V(r) = \frac{V + iW}{1 + e^{\frac{(r-a)}{a}}}$$

more satisfactory than a square well.

The region intermediate in energy between the work of Feshbach, Porter and Weisskopf (loc. cit.) and Fernbach, Serber and Taylor (loc. cit.) was investigated by Culler, Fernbach and Sherman (1956). They obtained good fits with elastic scattering and total cross section experiments performed using neutrons with an incident energy of 14 MeV by using both a square well and rounded well potentials.

A simple relation

$$\Im V_0 = \frac{\hbar}{\lambda m} (E + V_0)^{1/2}$$

was given by Francis and Watson (1953) to relate the magnitude of the imaginary part of the complex potential ($\Im V_0$) and the mean free path (λ) of a nucleon in nuclear matter in terms of the mass of the nucleon (m), its energy (E), and the real part of the potential (V_0).

Using this relation Morrison, Muirhead and Murdoch (1955) obtained satisfactory values for the imaginary part of the optical potential from nucleon-nucleon scattering values. Similar results were obtained by Clementel and Villi (1955) and Lane and Wandel (1955).

Serber (1947) pointed out that after the first collision of a projectile with an energy of the order of 100 MeV with a nucleon of a complex nucleus the energy transfer to the nucleon of the nucleus will be of the order of 25 MeV. Consequently, the struck nucleon will not have a high probability of escape from the nucleus.

A nucleon which participated in the initial nucleon-nucleon collision within a nucleus may itself collide with another nucleon of the nucleus, and so there arises the possibility of a nucleon cascade within the struck nucleus. This model was developed by Goldberger (1948). His method consists of tracing individual nucleons through the nucleus and following each collision partner in turn. Owing to the large number of possibilities statistical methods are employed. Collisions are only considered which leave both collision partners with an energy higher than the maximum Fermi energy of the nucleus. (That is the

maximum energy that a nucleon in the nucleus might have in the stable state of the nucleus treating the nucleons of the nucleus as a Fermi gas). The path of each nucleon which has suffered a collision is followed until it has either escaped or has insufficient energy to penetrate the Coulomb barrier. Subsequent de-excitation of the nucleus is assumed to take place according to the evaporation theory of Weisskopf (1937).

Experiments performed by Hadley and York (1950) measured the energy and angular distribution of fast charged particles emitted from carbon, copper and lead on bombardment with neutrons with an energy of 90 MeV. The results indicated a large direct interaction. The more energetic emitted particles were found to be more forward peaked. The results were not in general in close agreement with the predictions of the Goldberger model.

To test the Goldberger model in more detail Bernardini, Booth and Lindenbaum (1952a) bombarded electron sensitive nuclear emulsions with protons and neutrons with an energy of the order of 400 MeV. About 80% of the events observed were due to reactions taking place in silver and bromine, the heavy nuclei of the

emulsion. The prong distribution, energy and angular distribution all appeared to be in general agreement with the Goldberger model.

The programme proposed by Goldberger of following individual nucleons through the nucleus was performed in later work by Bernardini, Booth and Lindenbaum (1952b) for incident particles with an energy of the order of 400 MeV. Monte Carlo methods were used to treat the complicated cascade. The results of this calculation were found to be in satisfactory agreement with experiment.

At lower energy the de Broglie wavelength of a nucleon becomes larger and so it might be expected that the Goldberger model would be less valid. To test the limit of this model an experiment and calculation similar to that of Bernardini et al. was performed by Morrison, Muirhead and Rosser (1953) for protons with an energy of 120 MeV. Evidence was found that particles emitted with energy as low as 20 MeV could perhaps be accounted for by the Goldberger model. However, their results at this energy tended to be obscure due to the large number of evaporation protons.

To investigate the possibility of a direct

nucleon-nucleon interaction within complex nuclei at rather low energies it was proposed to use neutrons with an energy of the order of 14 MeV as the bombarding particle. Perhaps the simplest experiment, from the theoretical standpoint, would be one of the type (n,n') since it would not involve Coulomb penetrability. However, the low efficiency for detecting neutrons ($\leq 5\%$) combined with the low fluxes ($\sim 10^7$ neutrons per second into 4π) which were available in Glasgow at that time ruled out this possibility.

The experiments of Paul and Clarke (loc. cit.) on (n,p) reactions using neutrons with an energy of 14 MeV indicated a direct interaction. However, the errors in this experiment were large while uncertainties existed as a result of Coulomb barrier penetrability and level densities. Since 1953 many experiments in this energy range, mainly on inelastic proton scattering, have confirmed a form of direct interaction. When the present series of experiments were started no results had been published on the angular distribution or energy spectra of protons or alpha particles from a reaction induced in complex nuclei by neutrons with an energy of the order of 14 MeV.

CHAPTER II

(n, α) REACTIONS IN COMPLEX NUCLEI

(i) Introduction

The experimental results of Paul and Clarke (loc. cit.) are very surprising. In this work values of (n,p) and (n, α) cross sections were found many times larger (in some cases 1,000 times larger) than the statistical model would predict. An attempt to explain the large (n,p) cross section was made by Austern et al. (1953) on the basis of direct interaction taking place at the nuclear surface. By assuming that scattering takes place near the surface of the nucleus, protons would have only part of the Coulomb barrier to penetrate in order to escape. Although this might explain the large values observed for (n,p) cross sections it is difficult to extend this explanation to (n, α) reactions. As a first approximation it would be necessary to postulate alpha particle subgroups within all nuclei, even very heavy nuclei.

Since direct interaction of some nature would be required to explain the large cross sections found by

Paul and Clarke the angular distribution would be expected to be forward peaked. Hence it was proposed to investigate the angular distribution of the alpha particles emitted from neutron induced reactions in heavy or medium heavy nuclei.

The main disadvantage of experiments employing nuclear emulsions is the long scanning time usually required. In order to minimise scanning time it is desirable to have a simple geometric condition which may be applied to the tracks being investigated. If an external radiator is used then only tracks entering at the emulsion surface need be considered. In the case of alpha particles a very thin radiator is required to minimise energy loss. Since reactions in which alpha particles are emitted might be expected to have small cross sections, partly due to the Coulomb barrier, it is difficult to have a comparable number of "interesting" tracks and background.

(ii) (n, α) Reactions In Emulsion Nuclei

Although reactions can take place when a nuclear research emulsion is bombarded with neutrons with an energy of the order of 14 MeV which involve both singly

and doubly charged particles, it is possible to distinguish alpha particles from singly charged particles. However, since only alpha particles arising from (n,α) reactions in heavy nuclei were to be investigated it was necessary to obtain a method of distinguishing these alpha particles from (n,α) reactions in other nuclei. In a few cases after a charged particle has been emitted from a nucleus in which a neutron induced reaction has taken place the residual nucleus is radioactive and decays by emission of a beta particle. If electron sensitive nuclear emulsions are used the beta particle from the radioactive decay will be detected. The decay electron also indicates unambiguously the direction of the alpha particle.

The composition of an Ilford G.5. electron sensitive nuclear research emulsion is given in table 1.

Table 1

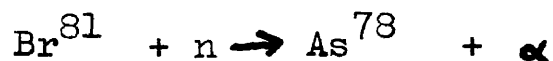
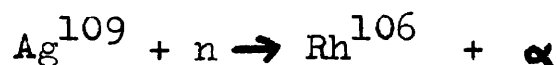
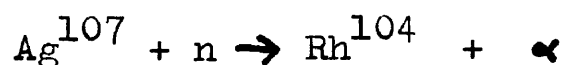
Composition of Ilford G.5. emulsion

Element	gm/cm ³
Silver	1.85
Bromine	1.34
Iodine	0.024
Sulphur	0.010
Carbon	0.27
Nitrogen	0.067
Oxygen	0.27

After an (n, α) reaction in the lightest nuclei of the emulsion (carbon, nitrogen and oxygen) the final nucleus is stable. Only 4.2% of the sulphur nuclei occurring in natural sulphur after an (n, α) reaction decay by emission of a beta particle. Since very little sulphur is present in a nuclear research emulsion few sulphur atoms will be observed to have an electron and an alpha particle coinciding at the position of the original nucleus. Similarly because of the small amount of iodine present, nuclei of this element may be neglected.

Natural silver consists of 52% Ag^{107} and 48% Ag^{109} and natural bromine consists of 49% Br^{81} and 51% Br^{79} .

(n, α) reactions in these nuclei are described by



Since the half life of As^{78} is 90 minutes many of the alpha particles arising from Br^{81} will have an electron at their origin. The half life of As^{76} is 26.8 hours, and so if development takes place a few hours after the exposure virtually no electrons from this reaction will be observed.

Both Rh^{104} and Rh^{106} are beta active isomeric nuclei with half lives of 4.4 minutes, 42 seconds, and 2 hours and 30 seconds respectively. Hence if processing commences a few hours after the exposure it is possible to distinguish (n, α) reactions originating in Ag^{107} , Ag^{109} and Br^{81} from other (n, α) reactions.

The cross section obtained by Paul and Clarke (loc. cit.) using neutrons with an energy of 14 MeV for an (n, α) reaction in Br^{81} was 103 mb that is 572 times larger than was predicted on the basis of the statistical model.

(iii) Exposure and Development of Emulsions

Ilford G.5. nuclear research emulsions 400 microns thick and 2"x2" in area on glass backings were used. These emulsions were exposed to neutrons with an energy of 14 MeV from the $\text{T}(d, n)\text{He}^4$ nuclear reaction induced by deuterons accelerated on the Glasgow H.T. set. The tritium target consisted of tritium partly absorbed and partly chemically combined with zirconium. This was soldered to a brass water cooled backing and fitted to the H.T. set.

The neutrons entered the centre of the emulsion

at an angle of 30° to the emulsion surface. The exposure lasted two hours and the integrated neutron flux at the emulsion surface was 6.5×10^8 neutrons/cm².

Three hours were allowed to elapse between the end of the exposure and the start of the developing process. The developing process consisted of first placing the emulsions in a dish of water at 20°C and then lowering the temperature rapidly to $\sim 5^{\circ}\text{C}$. At this temperature the emulsion is insensitive to charged particles and so any radioactive decays which took place after the start of the developing process were not recorded.

The method employed for processing was essentially that proposed by Dainton, Gattiker and Lock (1951). This method is described in table 2. Care was taken that the emulsion never suffered a rapid change in temperature after the initial lowering to 5°C . Before being placed on the hot plate excess developer was carefully removed from the emulsion surface by filter paper. The remaining cold stages were performed in large dishes standing in a trough of cold water supplied by a cooling unit.

The thickness of the emulsion and glass backing was measured before and after processing. These readings together with the thickness of the emulsion measured on

Table 2

Developer: Amidol 3 gm, Anhydrous sodium sulphite 12 gm,

Distilled water 1000 cc.

Stop bath: $\frac{1}{2}\%$ Acetic acid.

Fix: Sodium thiosulphate 400 gm, Sodium bisulphite 30 gm,

Tap water 1000 cc.

TreatmentTime

Pre soak	90 minutes
Developer 5°C	90 minutes
Hot plate 20°C	30 minutes
Stop bath 10°C	90 minutes
Wash, distilled water 5°C	90 minutes
Fixing 5°C	36 hours
Wash 5°C	60 hours
Drying	60 hours

a microscope after processing gave the thickness of the emulsion during the exposure.

Scanning was performed using a Watson binocular microscope with x10 eyepieces and a x45 oil immersion objective. To facilitate scanning a graticule was placed in one eyepiece. A volume at the centre of the emulsion was scanned for alpha particles and electrons appearing to originate at the same point. All tracks which appeared to satisfy this condition were further examined by means of a x90 oil immersion objective. Only tracks having dips of both electron and alpha particle of less than 45° in the unprocessed emulsion were recorded.

The scanning was made difficult by the large background and the small number of events found, the latter indicating a much smaller cross section than that reported by Paul and Clarke (loc. cit.). The small cross section found in the present experiment led to the abandoning of the attempt to obtain an angular distribution and the cross section for the process was calculated.

(iv) Calculation of the Cross Section

Since tracks with dips of both electron and alpha particle of less than 45° were accepted, $(\frac{1}{\sqrt{2}} \times \frac{1}{\sqrt{2}}) = \frac{1}{2}$ of the desired type of track in the volume scanned were recorded. Since the exposure lasted two hours and the time after the exposure to the start of the developing process was three hours virtually no events originating in Br^{78} were recorded. Hence only the reactions $\text{Br}^{81}(n, \alpha)\text{As}^{78}$, $\text{Ag}^{109}(n, \alpha)\text{Rh}^{106}$ and $\text{Ag}^{107}(n, \alpha)\text{Rh}^{104}$ contributed to the events observed. The fraction of nuclei of As^{78} which decayed before processing was 0.84. Since 36 events were found in a volume $0.82 \times 10^{-3} \text{ cm}^3$, and if it is assumed that the cross section for an (n, α) reaction in Ag^{107} , Ag^{109} and Br^{81} are equal, then each has a cross section of 9 ± 5 mb. The error shown allows the neutron flux to be in error by 50%.

A small volume of the emulsion was examined for protons with an energy and angle to the incident neutron direction satisfying the condition for the collision of neutrons with an energy of 14 MeV with the hydrogen of the emulsion. (Such tracks will be referred to in the following as 'knock-on protons'). Although no systematic scanning for knock-on protons was carried out,

the preliminary investigation indicated that such scanning would give the same integrated neutron flux as the scintillation monitor to within 50%. Hence the (n,α) cross section reported here is ten times smaller than the value reported by Paul and Clarke (loc. cit.).

The calculated cross section for an (n,α) reaction in Br^{81} on the basis of the statistical model is 0.2 mb according to these authors. Although the present results do not agree with those reported by Paul and Clarke they do not eliminate the possibility of direct interaction.

Because of the small cross section it is not possible to obtain the angular distribution by the method described here without an excessive amount of work.

(v) Further (n,α) Studies by Other Workers

During the course of the work described above, and since the completion of it, a number of results have been reported on cross sections for (n,α) reactions induced by neutrons with an energy of the order of 14 MeV.

The cross sections obtained for medium heavy and heavy nuclei are of the order of 10 mb and less. Blosser et al. (1955) obtained cross sections of the order of 4 mb for Zn^{68} , Zr^{90} , Zr^{94} and In^{115} using counters and chemical separation. Similar cross sections have been obtained by Armstrong and Brolley (1955), Ribe and Davis (1955), Dzantiev et al. (1957) and others. None of these workers have studied the elements investigated here.

CHAPTER III

(n,p) REACTIONS IN NATURAL ALUMINIUM AND RHODIUM

(i) Introduction

To investigate the possibility of a direct nucleon-nucleon interaction within complex nuclei at low energy, as suggested by the experiment of Morrison et al. (1953) it was proposed to study the (n,p) reaction using neutrons with an energy of the order of 14 MeV as the bombarding particle. The results of Paul and Clarke (loc. cit.) for an (n,p) reaction were in general larger than the cross section for an (n, α) reaction. This is of course the result that would be expected because of the lower Coulomb barrier for protons. The larger cross section for an (n,p) reaction together with the neutron flux available, although allowing the use of an external radiator was not sufficient for a collimated neutron beam to be used.

(ii) Apparatus

The apparatus is shown schematically in figure 2. The scattering camera consisted of a cylindrical brass

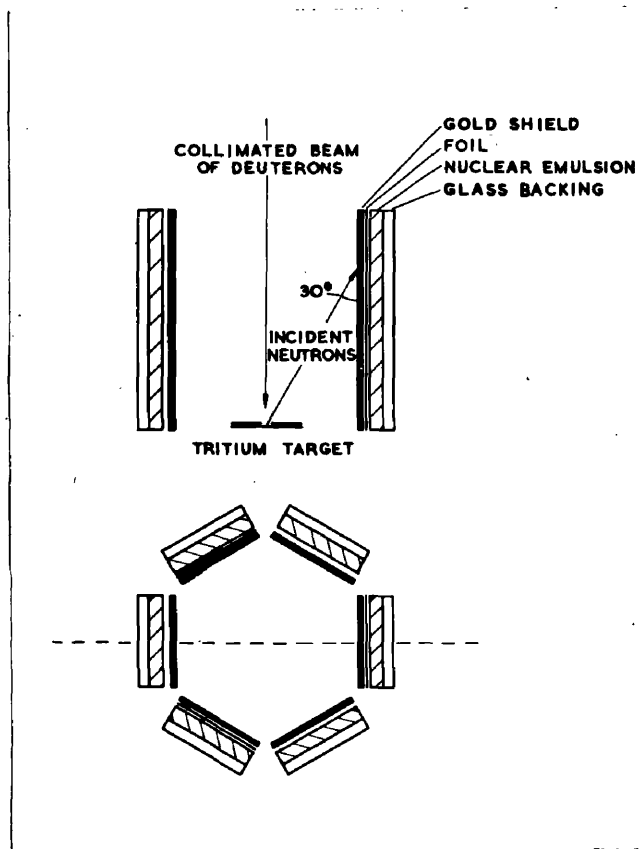


Figure 2 Schematic diagram of apparatus

container 5" in diameter and $5\frac{1}{2}$ " long. In the centre of the base was a water cooled block on which was placed a tritium zirconium target. The target was held in position by a cover plate, which was attached to the water cooled block by three small screws. In the centre of the cover plate was a hole $1/16$ " in diameter so giving an effective point source of neutrons.

A plate holder of brass screwed into the base of the brass cylinder. The plate holder was capable of holding six nuclear emulsions 4×1 " standing on end hexagonally around the tritium zirconium target. To minimise scattering the top of the plate holder was joined to the lower part by six thin brass rods. The deuteron beam was collimated by a brass plate at the top of the scattering camera with a hole 3mm in diameter in the centre. Beyond the collimating slit there was a liquid air trap $9\frac{1}{2}$ " long. The whole apparatus was joined to the column of the H.T. set. The air pressure in the scattering camera was that of the column of the set.

The material being investigated was placed between 400 micron thick sheets of gold and 400 micron thick Ilford C.2. nuclear research emulsions. The thickness of material used was aluminium 6 mg/cm^2 and rhodium 12 mg/cm^2 .

The aluminium was in the form of foil while the rhodium was electroplated on to the gold sheets. Background exposures were also obtained in which a 400 micron thick sheet of gold alone was placed above the emulsion.

(iii) Examination of Emulsions

Emulsions exposed to gold and the element being investigated and emulsions exposed only to gold were scanned in a region corresponding to neutrons incident at an angle of 30° to the unprocessed emulsion surface for proton tracks entering at the surface. The position of scanning corresponds to neutrons with an energy of 13.2 ± 0.2 MeV. Because of subsequent energy corrections and scanning efficiency only tracks with dips between 10° and 45° to the unprocessed emulsion surface were accepted.

Background effects present were due to tracks from the gold foil and tracks starting within the emulsion but unresolvable from tracks entering from outside. In order to obtain the energy and angular distribution of tracks arising in the gold scanning was performed inside the emulsion. To ensure that most of the tracks found within the emulsion stopped in the emulsion only the top half of the emulsion was scanned. The geometrical

acceptance conditions applied to tracks found within the emulsion was the same as those applied to the surface scanning, that is tracks were only recorded with dips between 10° and 45° to the unprocessed emulsion surface.

(iv) Analysis

Tracks found on the surface of the emulsion exposed only to gold and tracks found in the volume scanning were divided into two groups. One group consisted of knock-on protons, the other consisted of all other tracks. Using for normalisation the knock-on protons it was found that there were relatively more tracks other than knock-on protons on the surface than inside the emulsion. These excess tracks were assumed to be due to gold.

It was first assumed that all tracks satisfying the knock-on condition observed on the surface of the background plates do actually arise within the emulsion. Using these tracks and the knock-on protons found in the volume scanning for normalisation the energy and angle of tracks arising in the gold, other than those satisfying the condition for knock-on protons, was found. To allow for tracks originating in the gold and

satisfying the condition for knock-on protons a few tracks were added to the other gold tracks to give a smooth energy and angular distribution of tracks from gold. The energy of these tracks was modified according to the tracks dip in unprocessed emulsion to give the spectra expected from gold after the particles had passed through the material being investigated.

In table 3 is shown the number of tracks entering the surface of the emulsion exposed to gold and the material being investigated ('Protons observed'), the number of these found to be knock-on protons ('knock-ons'), the number due to other optically unresolvable background within the emulsion ('Background') and the number due to gold ('Gold'). The last column gives the number of tracks from the material being investigated.

Table 3

Allocation of tracks

Element	Protons observed	Knock- ons	Background	Gold	Protons from foil
Al	1600	220	30	70	1280
Rh	1140	490	60	90	500

Table 4

Energy loss in Al and Rh foils in MeV

Dip angle of proton	Initial Energy of Proton in MeV							
	Al foil				Rh foil			
	3	6	9	12	3	6	9	12
15°	1.2	0.6	0.4	0.35	1.1	0.8	0.6	0.5
30°	0.5	0.25	0.2	0.15	0.4	0.3	0.25	0.2

The energy spectra and angular distributions of the protons from the material being investigated were found by subtracting according to energy and angle the total background from the tracks observed in the emulsion exposed to aluminium and rhodium.

All angular distributions and energy spectra were corrected for the geometry of the apparatus. Figure 3 shows the variation of the efficiency of the geometry used to detect protons from the foil as a function of the direction of the proton with respect to the incident neutron direction.

An error is introduced in the energy spectra due to the energy loss of protons in traversing the foil of the material being investigated. The energy loss is a function of proton energy and dip. The energy loss for a few typical proton energies is shown in table 4 for protons assumed to start at the centre of the foil.

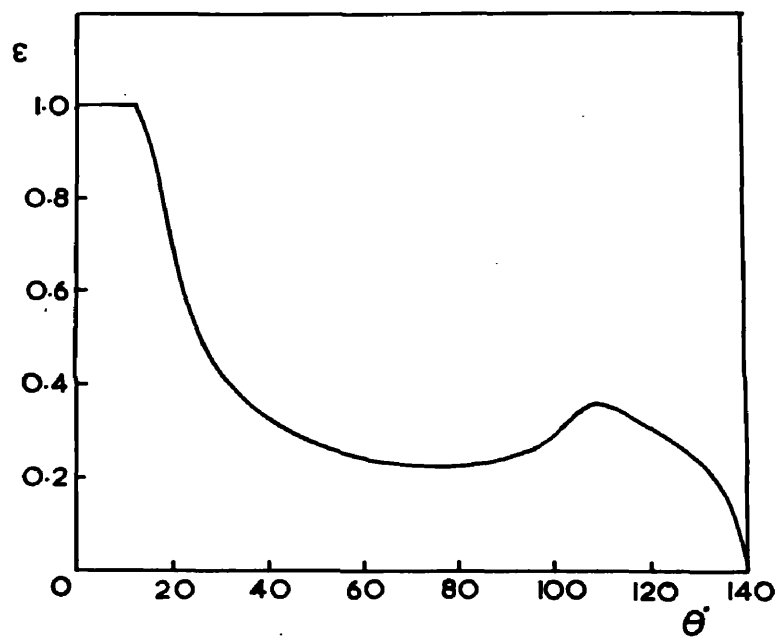


Figure 3 Geometrical efficiency (ξ) of apparatus as a function of angle (θ) to the incident neutron direction.

A method for correcting the energy spectra for the finite thickness of the target foil was suggested by G. Brown. In this method the target foil was considered as divided into three foils each assumed infinitely thin. A numerical trial and error method was applied to find the spectrum from each foil which would give the observed energy spectrum. Unfortunately this method suffers from the disadvantage of smoothing the energy spectra. This method was applied to the aluminium energy spectrum.

As is indicated in table 4 the energy correction due to the finite thickness of the radiator becomes important at low proton energies. Since virtually no protons were observed from rhodium with an energy below 4 MeV the method of Brown, described above, was not applied. The rhodium energy spectra was simply corrected by adding to each track the energy it would have lost if it had started at the centre of the foil.

The integrated neutron flux was obtained from the volume scanning. Only tracks which satisfied the condition for knock-on protons were considered. The geometric acceptance conditions applied were the same as those used in the scanning for tracks entering the surface of the emulsion and so the geometrical correction

factors shown in figure 3 were used. Since neutron-proton scattering at an energy of 14 MeV is isotropic in the centre of mass system and the hydrogen content of an emulsion is known it was possible to calculate the integrated neutron flux at the centre of the emulsion surface which was scanned. The value obtained was used in calculating the differential cross section.

(v) Discussion of Aluminium and Rhodium Results

In the case of aluminium a number of short range tracks were found which were thought to be alpha particles. These were excluded from measurement.

Since natural aluminium consists of 100% Al^{27} and rhodium consists of 100% Rh^{103} , the investigation being described involved only one isotope of these elements.

The angular distribution obtained for the charged particles emitted (which shall be called for the present protons) when aluminium and rhodium are bombarded with neutrons with an energy of 13.2 MeV are shown in figures 4 and 5. The errors shown are the standard deviations. The angular distributions of the protons observed from aluminium were divided into three groups, namely protons of energy less than 4 MeV, those with an energy between 4

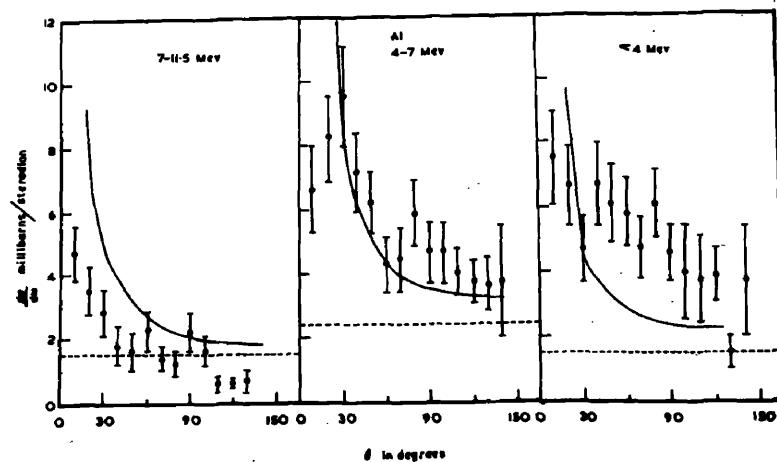


Figure 4 Angular distribution from aluminium.

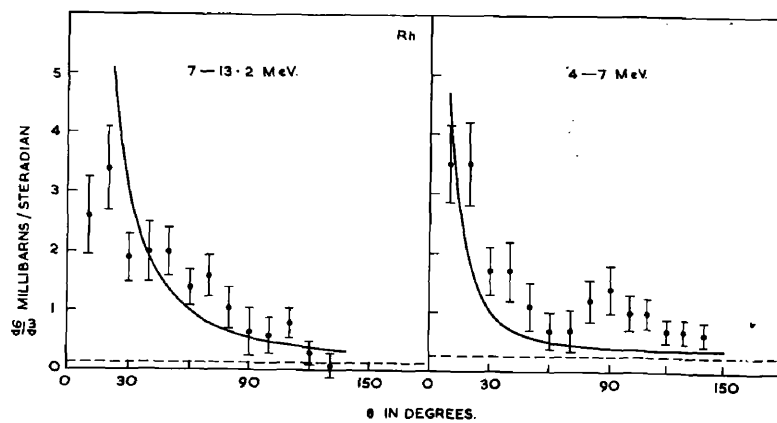


Figure 5 Angular distribution from rhodium.

and 7 MeV, and those of energy greater than 7 MeV. Since virtually no protons were found to be emitted from rhodium with an energy below 4 MeV the rhodium angular distribution is divided only into two.

The solid line is the angular distribution predicted by the model of Brown and Muirhead (1956). In this model the emission of protons is assumed to take place in two distinct stages. Initially the emission takes place due to direct nucleon-nucleon collisions occurring throughout the nuclear volume and later by the decay of the compound nucleus. They assumed that the target nucleus could be represented as a Fermi gas of nucleons and that direct collisions were limited by the Pauli exclusion principle. The dotted line is the isotropic contribution due to the decay of the compound nucleus according to the theory of Brown and Muirhead.

The angular distribution of the protons from rhodium is more forward peaked than that observed for the protons arising in aluminium. Protons of energy greater than 7 MeV are forward peaked for both aluminium and rhodium, protons of lower energy from aluminium are more, if not, isotropic within the present statistics. The distribution according to the theory of Brown and Muirhead (loc. cit.)

agrees with the rhodium data better than the aluminium. This theory appears to give a forward peak more pronounced than is indicated by the aluminium experimental results.

Figures 6 and 7 show the experimental energy spectra observed from aluminium and rhodium. In neither case has the energy spectrum the Maxwellian shape predicted by the statistical model. The energy spectra of the protons from aluminium and rhodium differ markedly in shape. The aluminium energy spectrum shows a high peak at low energy, that is for protons with an energy less than 5 MeV, while most of the rhodium cross section is for protons with an energy between 5 and 10 MeV. Assuming a nuclear radius of $1.4 \times 10^{-13} A^{1/3}$ cm, where A is the mass number, the usual simple expression for the classical height of the Coulomb barrier gives 4.5 MeV and 10 MeV for aluminium and rhodium respectively. Thus for both elements a considerable part of the cross section is below the classical height of the Coulomb barrier.

There are two possible explanations of the large low energy peak found in aluminium. Since it is not possible to distinguish protons and deuterons in Ilford C.2. nuclear research emulsions the spectra may contain a considerable number of deuterons. Although the Q value for

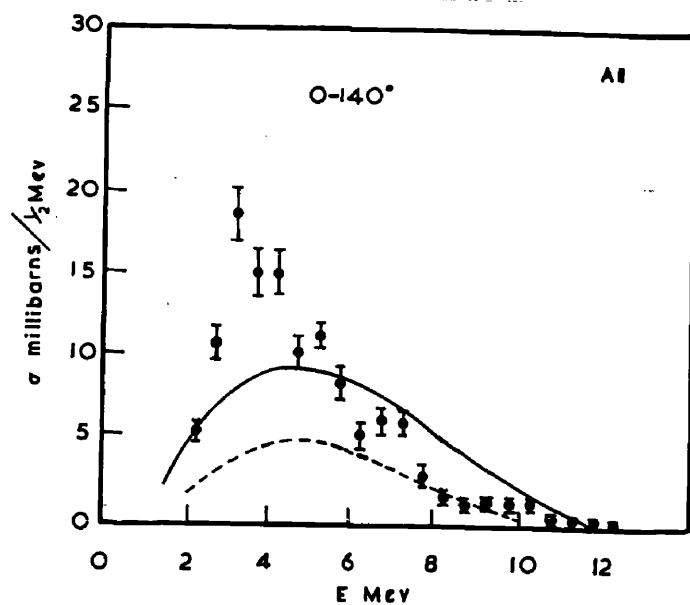


Figure 6 Energy spectrum from aluminium

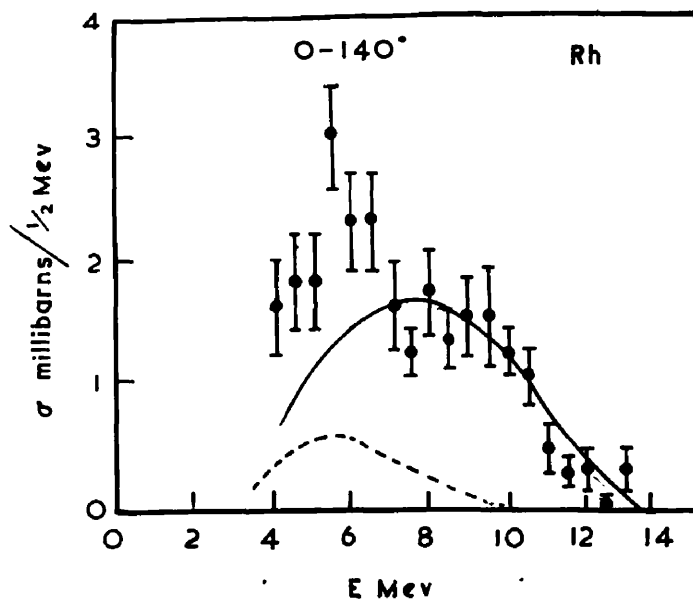


Figure 7 Energy spectrum from rhodium

an (n,d) reaction in aluminium is -6.09 MeV and for an (n,p) reaction is -1.09 MeV it does not necessarily follow that fewer deuterons than protons would be observed. (All Q values were obtained using the binding energy tables of Feather, 1953. These results are in substantial agreement with all later work on experimental mass value determinations for the elements investigated in this thesis). The higher Coulomb barrier for deuteron than proton emission will also not restrict appreciably the number of deuterons observed if the (n,d) reaction takes place by a pick-up mechanism at the nuclear surface. The number of deuterons emitted from aluminium will be discussed further in Chapter V. Since the Q value for an (n,d) reaction in rhodium is -4.25 MeV a number of deuterons may also be present in the spectra observed from this element.

A second explanation of the large number of low energy protons found in the case of aluminium may be obtained by considering the Q values for the processes (n,np) and (n,2n). Because of the Coulomb barrier it is expected that the probability of neutron emission is much greater than the probability of proton emission from a compound nucleus at the same excitation, assuming both processes to be energetically possible. However, it is

possible that for certain nuclei at a given excitation there exists Q values forbidding neutron emission, but allowing proton emission. This situation arises in the case of aluminium where the Q value for (n,np) is -8.3 MeV and for $(n,2n)$ is -13.0 MeV. Hence if after the emission of the first neutron the excitation energy of the aluminium nucleus is less than 4.7 MeV only proton emission can take place.

These mechanisms have not been considered in the theory of Brown and Muirhead (loc. cit.) and offer an explanation of the discrepancy between the results of their theory and experiment at low energies.

With the experimental arrangement used in the investigation being described the angular distribution was obtained for protons emitted in the angular range from 0° to 140° with respect to the incident neutron direction. It was assumed that the differential cross section was constant in the angular range from 90° to 180° and so the total cross section was obtained. The values obtained were 140 ± 30 mb and 25 ± 5 mb for aluminium and rhodium respectively.

The cross section obtained for aluminium may be compared with the results of Allan (1957), working at

Harwell. He measured the cross section for the emission of protons when aluminium is bombarded with neutrons with an energy of 14 MeV using nuclear research emulsions and obtained a value of 140 mb. This cross section was measured at an angle of $34^{\circ} \pm 20^{\circ}$ to the incident neutrons in the forward direction and so this value would be expected to be higher than the value reported here.

The cross section for $\text{Al}^{27}(\text{n},\text{p})\text{Mg}^{27}$ was measured by Paul and Clarke (loc. cit.) and by Forbes (1952) using an activation technique. They measured the residual activity of the Mg^{27} nuclei after the bombardment of aluminium with neutrons with an energy of the order of 14 MeV. Paul and Clarke obtained the value 52 ± 10 mb and Forbes the value 82 ± 5 mb.

If certain plausible assumptions are made concerning compound nucleus decay it is possible to obtain a value of the activation cross section from the energy spectrum reported here. If a compound nucleus is formed by the capture of a neutron with an energy of the order of 14 MeV after the emission of the first proton the nucleus might still have considerable excitation energy. Since the half life against γ decay is very long compared to the half life against particle emission, a particle will in

general be emitted provided such a process is energetically possible. Hence the area under the energy spectrum of the emitted protons where the nucleus has not sufficient energy to emit another particle might be expected to represent the activation cross section. The value obtained for the activation cross section from the energy spectrum reported here was 55 ± 15 mb in approximate agreement with the results of Paul and Clarke and of Forbes. The theoretical value for the activation cross section according to the calculation of Paul and Clarke for a pure statistical theory of the reaction is 146 mb.

The theory of Brown and Muirhead (loc. cit.) gives good agreement with the cross sections obtained experimentally. This theory predicts cross sections of 150 mb and 25 mb for aluminium and rhodium while the values obtained experimentally were 140 ± 30 mb and 25 ± 5 mb.

Results on the energy spectrum of protons emitted when rhodium is bombarded by neutrons with an energy of 14.5 MeV have recently been obtained by Colli et al. (1958) using counters. Although the energy spectrum obtained by these workers only covers the angular range 0° to 40° , and hence is not directly comparable with the present results, it follows closely the relatively

flat shape reported here.

The emission of protons from natural iron when bombarded by neutrons with an energy of 13.2 MeV was investigated by Brown and Morrison (Brown et al. 1957). This experiment also provided evidence for a direct interaction. A more detailed study of the protons emitted from the iron isotopes will be given in the next chapter.

Conclusions

There appears to be a contribution to the (n,p) reaction in aluminium and rhodium nuclei from a direct interaction process. The most conclusive evidence comes from the angular distribution of protons with an energy greater than 7 MeV. Many particles were found with an energy less than what might be expected to be the height of the Coulomb barrier in both cases. A portion of the low energy aluminium results might be explained by an (n,np) or (n,d) process.

CHAPTER IV

(n,p) REACTIONS IN Fe^{54} , Fe^{56} and Ni^{60}

(i) Introduction

The rhodium and aluminium results showed that a considerable fraction of the experimentally observed cross section could not be explained by a compound nucleus mechanism. Any type of direct interaction since it will involve individual nucleons might be expected to differ from nucleus to nucleus. However, because of uncertainties in the calculation of Coulomb penetrabilities, it is essential that any comparison of nuclei must be carried out for nuclei of similar or the same charge. It would be expected that owing to the large difference in the Q values for the (n,p) reaction in Fe^{54} (Q value 0.3 MeV) and Fe^{56} (Q value -2.9 MeV) that the contribution to the direct interaction in these nuclei would differ.

When the previous results were obtained there existed two theories pertaining to explain direct interactions in reactions induced by neutrons with an energy of the order of 14 MeV. In the model of Austern, Butler and McManus (1953) the direct interaction was assumed to be due/

due to collisions of the incident neutron with protons of the bombarded nucleus which had leaked through the Coulomb barrier. In this model the shape of the angular distribution depends on the angular momentum states involved. The second model, that of Brown and Muirhead, which was briefly described above, considered all particles to have the same Coulomb barrier to penetrate after the n-p collision. This model predicts rapid changes in the cross section with changes in the Q value for the process and ^{with} ~~on~~ level densities. As a result of these considerations this theory predicts markedly different cross sections and angular distributions for the two isotopes of iron Fe^{54} and Fe^{56} . A study of these nuclei would provide a test of this model.

The nuclei Fe^{54} and Fe^{56} also serve as a test of the assumption that the low energy peak in the energy spectra is the result of an (n,np) reaction. An (n,np) process not competing with an (n,2n) process is possible in Fe^{54} , but not in Fe^{56} . Because of the similar Coulomb barriers the occurrence of such a peak in Fe^{54} and not in Fe^{56} would serve as almost conclusive evidence for an (n,np) type of reaction. Since it was hoped in the present investigation to obtain better statistics than

in the aluminium and rhodium experiment it would be possible to measure the angular distribution of the low energy peak.

The nucleus Fe^{56} was also thought to be of interest because of an approximately rectangular energy spectrum found by Allan (1957) for protons emitted from Fe^{56} on bombardment with neutrons with an energy of 14 MeV. He did not measure the angular distribution of the protons.

After the completion of the Fe^{54} and Fe^{56} work it became clear that a study of the reaction $\text{Ni}^{60}(\text{n},\text{p})\text{Co}^{60}$, which has a Q value of -2.0 MeV, that is intermediate between Fe^{54} and Fe^{56} , but has an approximately similar Coulomb barrier, would be of interest. Since the experimental arrangement and analysis was very similar to that used for Fe^{54} and Fe^{56} the investigation of all three isotopes will be described simultaneously.

(ii) Apparatus, Exposure, and Development of Emulsions

Since no higher neutron fluxes were available the apparatus used in this investigation was the same as that used in the previous work except that the liquid air trap separating the scattering camera from the H.T. set was omitted. To improve energy resolution it was

proposed to use thinner foils ($\sim 6 \text{ mg/cm}^2$) than that used in the rhodium experiment ($\sim 12 \text{ mg/cm}^2$). In the present exposure the 200 KeV Glasgow H.T. set was employed.

Separated isotopes of Fe^{54} , Fe^{56} and Ni^{60} each of thickness 7 mg/cm^2 covering an area $1\frac{1}{2} \text{ cm} \times 1\frac{1}{2} \text{ cm}$ were supplied by Harwell electroplated on to 5 micron thick gold. The composition of the isotopes were:
 Fe^{54} separated isotope consisted of 67% Fe^{54} and 23% Fe^{56} ,
 Fe^{56} separated isotope consisted of 99.9% Fe^{56} , and
 Ni^{60} separated isotope consisted of 99.2% Ni^{60} . These gold foils were placed on top of 400 micron thick sheets of fine gold 4"x1" in such a position as to correspond to neutrons incident on the separated isotopes at an angle of 30° when the gold sheets were placed in the scattering camera. The gold was placed on top of 400 micron thick 4"x1" Ilford C.2. nuclear research emulsions with the separated isotope next to the emulsion. Since iron and nickel attack nuclear emulsions it was essential that they be kept apart from the emulsion surface. This was done using 5 micron diameter platinum wires placed between the emulsion and the separated isotope one at the top the other at the bottom of the foil. To protect the emulsion from the light generated by gas scattering

of the deuteron beam the glass backing of the emulsion was covered by black tape.

In each exposure four foils of two of the separated isotopes and two emulsions exposed only to gold were placed in the scattering camera. They were arranged alternately in the hexagonal plate holder. Great care was taken that the emulsion surface was perpendicular to the plane of the tritium target.

The deuteron current falling on the water cooled block was measured throughout the exposure. A plastic scintillator and photomultiplier placed 100 cm from the neutron source was used to monitor the neutron flux. The scattering camera was adjusted to give the maximum current falling on the water cooled block while the scintillation counter gave the integrated neutron flux.

In the last of the three Fe^{54} , Fe^{56} exposures and in all the Ni^{60} exposures, which were scanned, the scintillator spectrum was observed on a kicksorter and the bias of the discriminator set so as to record pulses due to knock-on protons from neutrons with an energy of the order of 14 MeV. This was found to be necessary due to large differences in scintillation counter fluxes and the fluxes observed by emulsion scanning in the first

two exposures. The excess low energy neutrons appeared to be due to the $d(d, \text{He}^3)n$ reaction. Before all exposures the whole apparatus was thoroughly cleaned to remove deuterium deposited in previous exposures. The deuterium deposit on the water cooled block and collimating slit was large due to difficulty in focussing the deuteron beam.

An integrated neutron flux of a few times 10^8 neutrons/cm² at the emulsion surface was aimed at in all exposures.

The H.T. set operated during the exposures at a deuteron energy of 170 KeV.

The thickness of the emulsion and glass backing of all plates was measured immediately on removing the scattering camera from the column of the H.T. set in order that the emulsion thickness could be obtained under conditions as close to those in which the experiment was performed as possible.

The method used for processing was the same as that used previously, except that it was necessary to add an additional stage. After the usual developing process and when the dilution of the fix reached the stage when fix could not be detected by a potassium permanganate

solution the emulsions were placed in a 2% glycerine solution for one hour. This prevented the emulsions becoming too dry and brittle and so peeling off the glass backings.

This method was found to give clear, evenly developed emulsions with a low level of distortion.

Thickness measurements were performed after the emulsions were dry with a comparitor, reading to at least one micron, and a Cooke M 4000 microscope to the same accuracy in order that the shrinkage factor of the emulsion could be obtained at any subsequent time.

(iii) Examination of Emulsions

Areas of emulsion surface corresponding to neutrons incident at an angle of 30° to the emulsion surface on all plates were examined. The area of scanning on each plate was chosen so small that the incident neutron direction was never in error by more than 3° . The energy of the incident neutrons was 13.5 ± 0.2 MeV.

In order that the scanning efficiency would be as high as possible the scanning was performed in two stages. First the emulsions were examined with x50 oil immersion objectives and x10 eyepieces with a graticule and the

coordinates of all fields of view in which a track appeared to cross the emulsion surface were recorded. The position of the track within the field of view was also noted together with a rough drawing of the track. This was performed for a whole "scan" (usually 6 mm in length) without stopping to examine any track in detail. By moving a grain on one side of the graticule to the other the microscope stage was moved one graticule size (90 microns) at a time. The graticule square was divided into four by the horizontal axis and the graticule scale. On the emulsions exposed to Fe^{54} , in which the density of tracks crossing the emulsion surface was much greater than in any of the other exposures, each square of the graticule was examined separately. With this method an efficiency of at least 98% was achieved.

On completion of a scan the tracks recorded were examined in more detail as to their direction. Those tracks which appeared to enter at the emulsion surface were further examined by means of a x90 oil immersion objective to determine whether or not they actually entered at the surface. It was possible to decide in very nearly all cases if the track started at the emulsion surface to within $\frac{1}{2}$ micron, that is to the diameter of an emulsion grain. This examination of tracks was performed by physicists to standardise selection criteria. Agreement as to whether or

not the tracks entered at the surface was obtained in all cases. It was found difficult to decide in which direction a few short range tracks were travelling. (These tracks correspond to protons in the energy range 2-4 MeV). A similar number of such tracks was observed in emulsions exposed to gold and to gold and separated isotope.

Since it was difficult to tell in which direction very short range tracks were travelling no tracks with projected length less than $22\frac{1}{2}$ microns were measured. This limit corresponds to protons with an energy of 1.5 MeV. Because the scanning efficiency decreases for steep tracks an upper limit of 45° in the unprocessed emulsion was imposed on the dip angle. To eliminate the possibility of large uncertainties in the energy of tracks passing through large distances of foil no tracks were accepted with a dip angle of less than 10° to the emulsion surface.

Tracks which satisfied the above conditions were accepted for measurement. All measurements were made using x50 oil immersion objectives. The projected direction of the point of entering the emulsion on the plane of the emulsion with respect to the sides of the emulsion was measured with a goniometer eyepiece (horizontal angle). The projected length on the emulsion surface of the track was also

measured. The depth in the emulsion of the first 45 microns projected length was measured. The depth in the processed emulsion of the end of each accepted track was measured and so also was the position of any sharp discontinuities in the dip of the track. The thickness of the emulsion was measured with a microscope each day.

Volume scanning was performed in which a given volume of emulsion was searched for the start of proton tracks. Great care was taken that no tracks were missed. This was done by considering only $\frac{1}{4}$ of the field of view at a time. The volume scanning was somewhat easier than in the aluminium and rhodium exposures due to less fogging of the emulsion. The efficiency for detecting protons starting within the emulsion was greater than 95%. Tracks which satisfied the same geometric conditions as applied to the surface scanning were measured by the method described above.

(iv) Analysis of Tracks

The angle which each track made with respect to the incident neutron direction was calculated. Horizontal angle measurements were made to within $\pm 2^\circ$ and the dip angle in the processed emulsion was correct to within $\pm 4^\circ$ and so the angle with respect to the incident neutron direction

was correct to within $\pm 5^\circ$ in all cases.

The total dip along with the projected length and details of any sharp changes in the dip were used to calculate the energy of the accepted tracks assuming the tracks to be protons. In the energy calculation the range energy tables of Rotblat (1951) were used.

Figure 8 shows the distribution according to energy and angle in space with respect to the incident neutron direction of tracks with an energy less than 4 MeV observed on a typical background plate. Very few proton tracks of energy greater than 4 MeV do not satisfy the condition for knock-on protons produced by neutrons with an energy of the order of 14 MeV. Figure 8 indicates that background tracks of energy less than 4 MeV can be divided into three groups of which the central group corresponds to knock-on protons produced by neutrons with an energy of the order of 14 MeV. A possible explanation of the other two groups, as suggested above, is that they are due to knock-on protons from the collision of neutrons with an energy of the order of 4 MeV produced in the reaction $d(d, \text{He}^3)n$. If this is the case it then appears that there are two sources of neutrons with an energy of the order of 4 MeV; one at the collimating slit, the other at the tritium target.

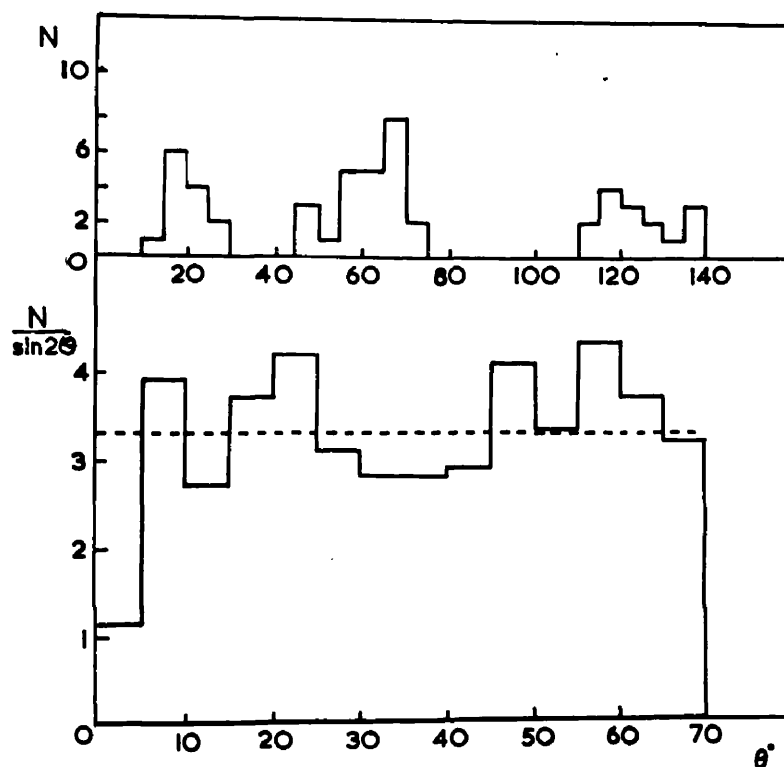


Figure 8 (Top) Number of protons (N , arbitrary units) observed with an energy < 4 MeV starting within the emulsion as a function of the angle (θ) to the incident neutron direction. (Bottom) Number of protons ($\frac{N}{\sin^2 \theta}$, arbitrary units) per unit solid angle in the centre of mass system as a function of the angle (θ) in the laboratory system to the incident neutron direction.

(v) Analysis of Results

Since the results of the aluminium and rhodium investigation indicated a cross section for the emission of protons from gold of 10 mb as an upper limit, it was decided in the present investigation to neglect the modification of the gold spectrum due to protons from gold passing through the separated isotope layer. These protons comprise only about 20% of the total background and the energy loss is small for most of these particles. Hence a straight subtraction of the background tracks from tracks observed in the emulsion exposed to the separated isotope was made according to space angle and energy. The total number of protons entering the emulsion surface from each isotope and the corresponding background subtractions are shown in table 5.

Table 5

Allocation of protons observed.

Isotope	Number of protons observed	Background	Number of protons from isotope
Fe ⁵⁴	1823	321	1502
Fe ⁵⁶	2479	1257	1222
Ni ⁶⁰	2498	792	1706

The thickness of the foil was taken into account by adding to each track, according to its dip in unprocessed emulsion, the energy it would have lost in penetrating half the thickness of the foil being investigated. The energy corrections applied to protons of various observed energies for an iron foil of thickness 7mg/cm^2 are given in table 6. The corrections for a nickel foil are very similar.

Table 6

Energy corrections for iron foils

Dip Angle	Observed energy of proton in MeV			
	3	6	9	12
15°	0.6	0.4	0.35	0.25
30°	0.35	0.2	0.15	0.15

The angular and energy distributions of the tracks observed to originate from the separated isotope foil were corrected for the geometry of the apparatus. An additional correction was applied to the low energy tracks due to the cut-off at projected lengths of $22\frac{1}{2}$ microns.

The volume scanning was used in the same way as in the aluminium and rhodium investigation to obtain the integrated neutron flux. Figure 8 shows the angular distribution of the knock-on protons from the collision of neutrons with an energy of 13.5 MeV observed in the volume

scanning. At an energy of 13.5 MeV the angular distribution of such protons is isotropic in the centre of mass system. The loss of tracks at large angles ($>70^\circ$) is due to the experimental cut-off at an energy of the order of 1.5 MeV on all tracks measured.

(vi) Angular and Energy Distributions

The angular distributions of the protons emitted from Fe^{54} , Fe^{56} and Ni^{60} are shown in figures 9, 10 and 11 for protons of energy 0-4 MeV, 4-7 MeV and greater than 7 MeV.

The energy spectra of protons emitted from Fe^{54} , Fe^{56} and Ni^{60} are shown in figures 12, 13 and 14 for the angular ranges 0° - 60° , 60° - 90° and 90° - 140° where the angles are measured with respect to the incident neutron direction. The first two angular intervals contain equal solid angles.

The solid line in figures 12, 13 and 14 is the proton distribution for an (n,p) reaction predicted on the basis of the statistical theory of Weisskopf and Ewing (1940). The variation of the level density with excitation energy was assumed to follow the formula given by Lang and Le Couteur (1954). In these calculations the cross sections for the formation of a compound nucleus given by Blatt and

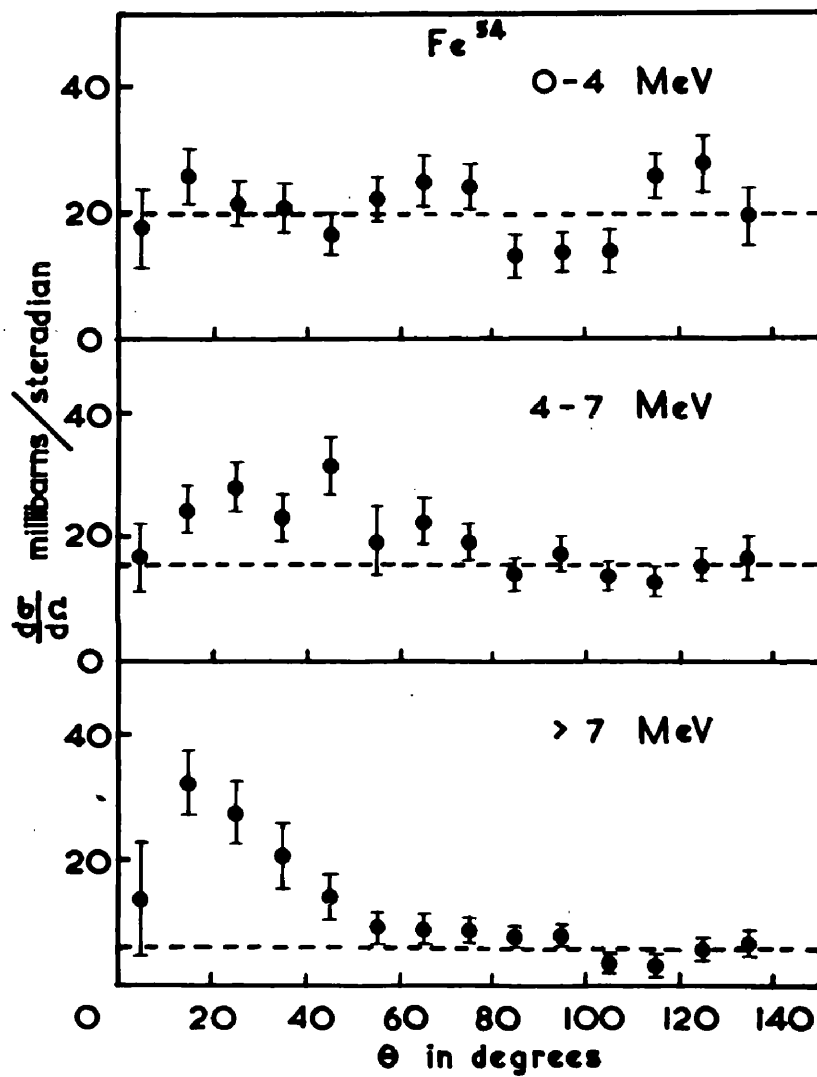


Figure 9 Angular distribution from Fe^{54}

N.B. In these and subsequent figures, the small connections to the centre of mass motion has been neglected.

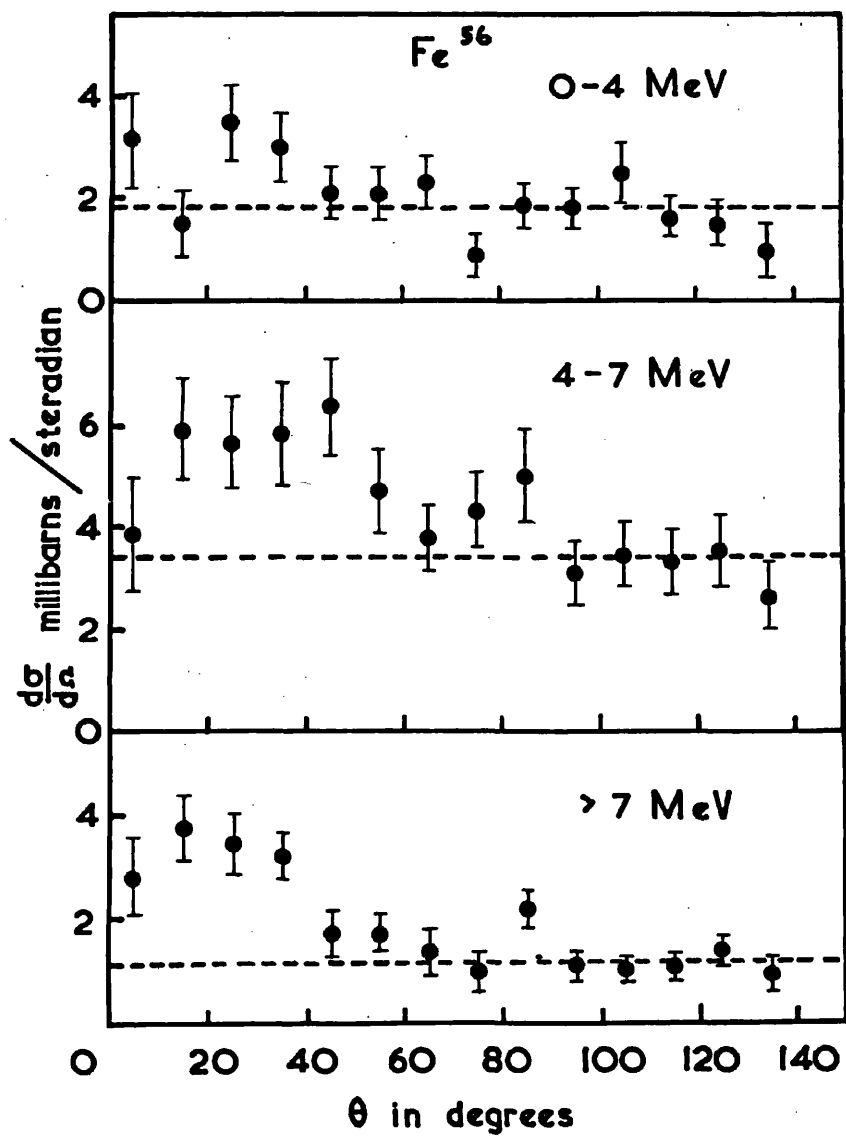


Figure 10 Angular distribution from Fe^{56}

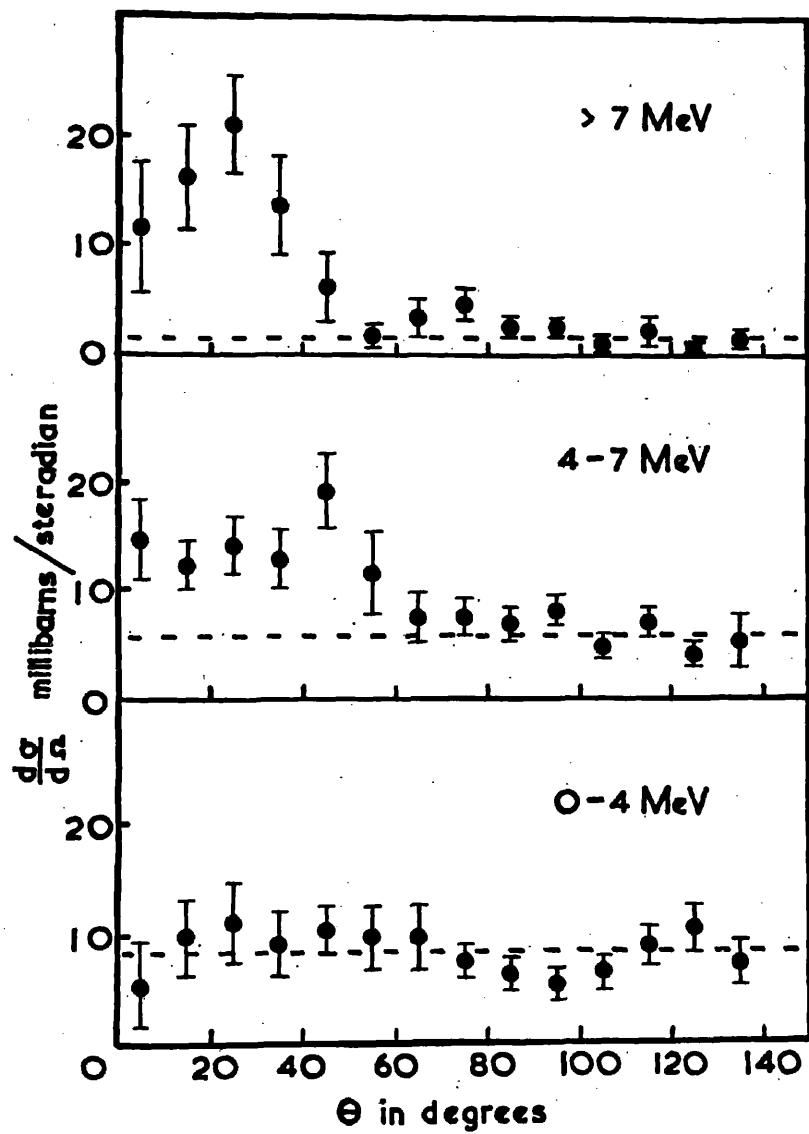


Figure 11 Angular distribution from Ni^{60}

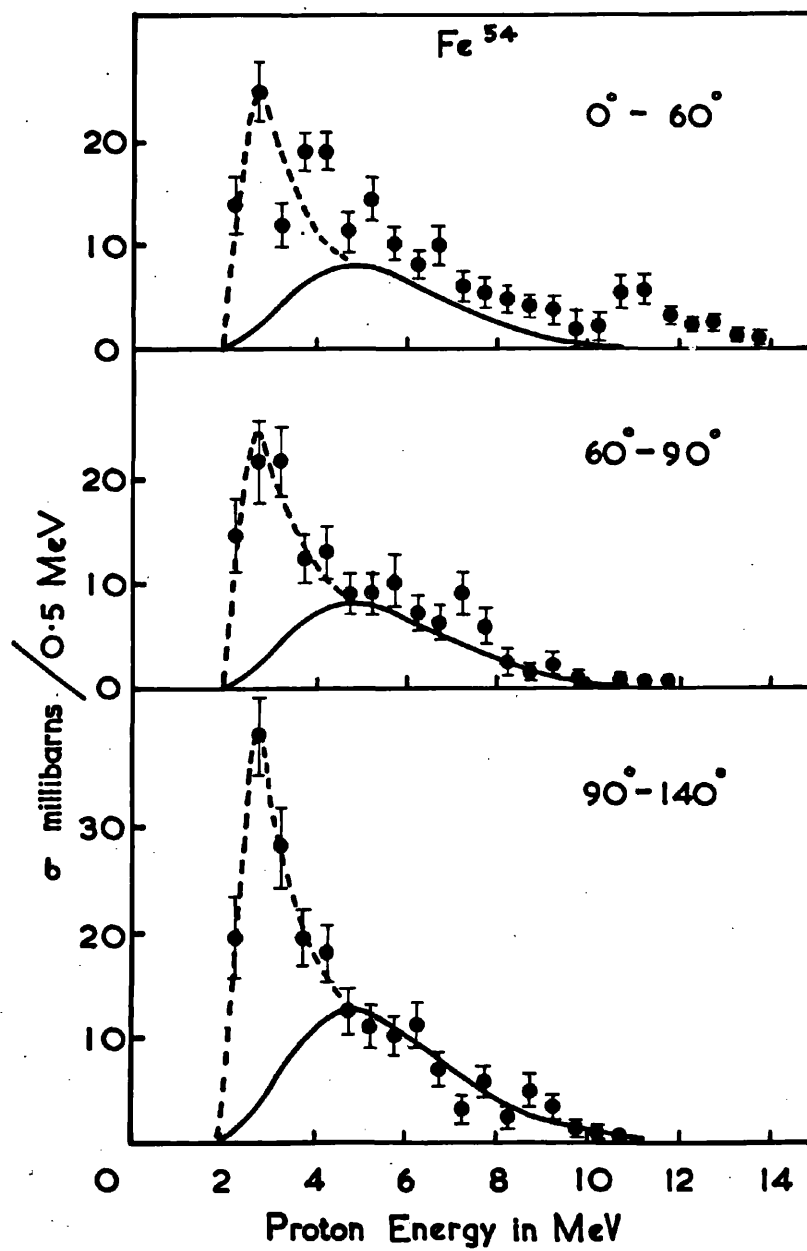


Figure 12 Energy spectrum from Fe^{54}

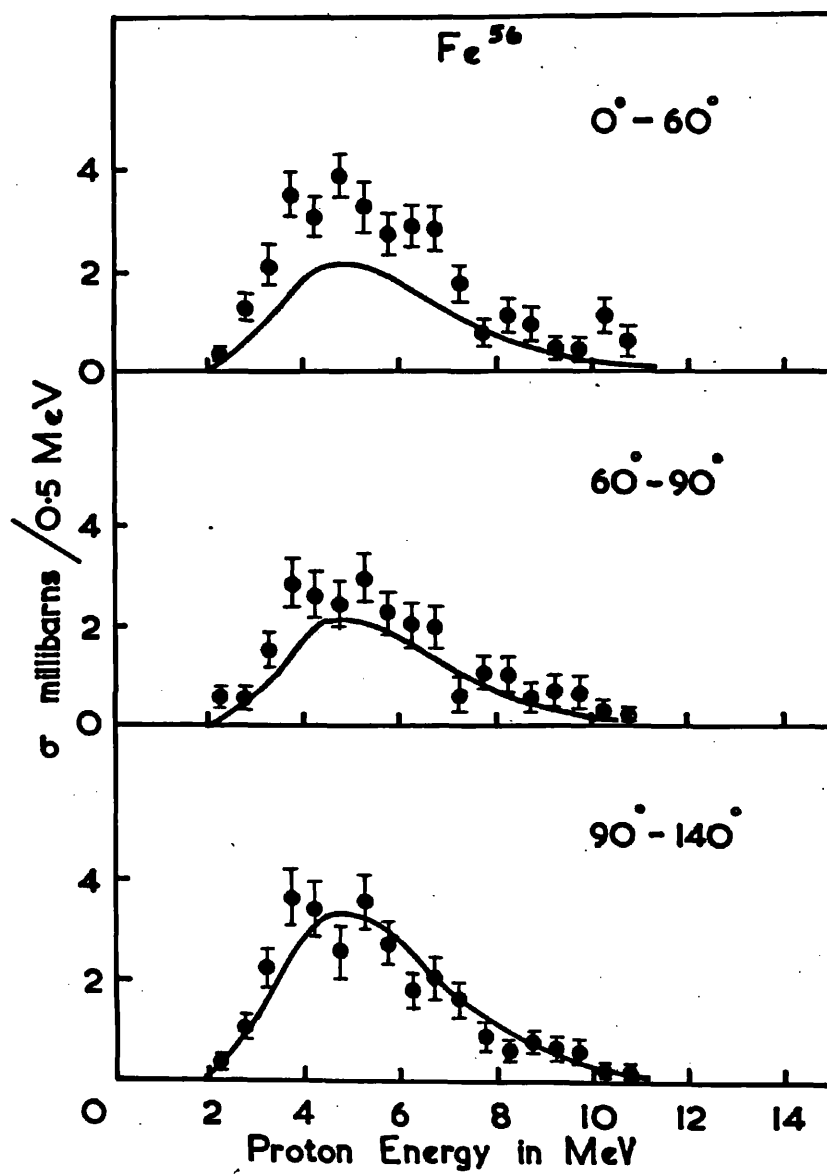


Figure 13 Energy spectrum from Fe^{56}

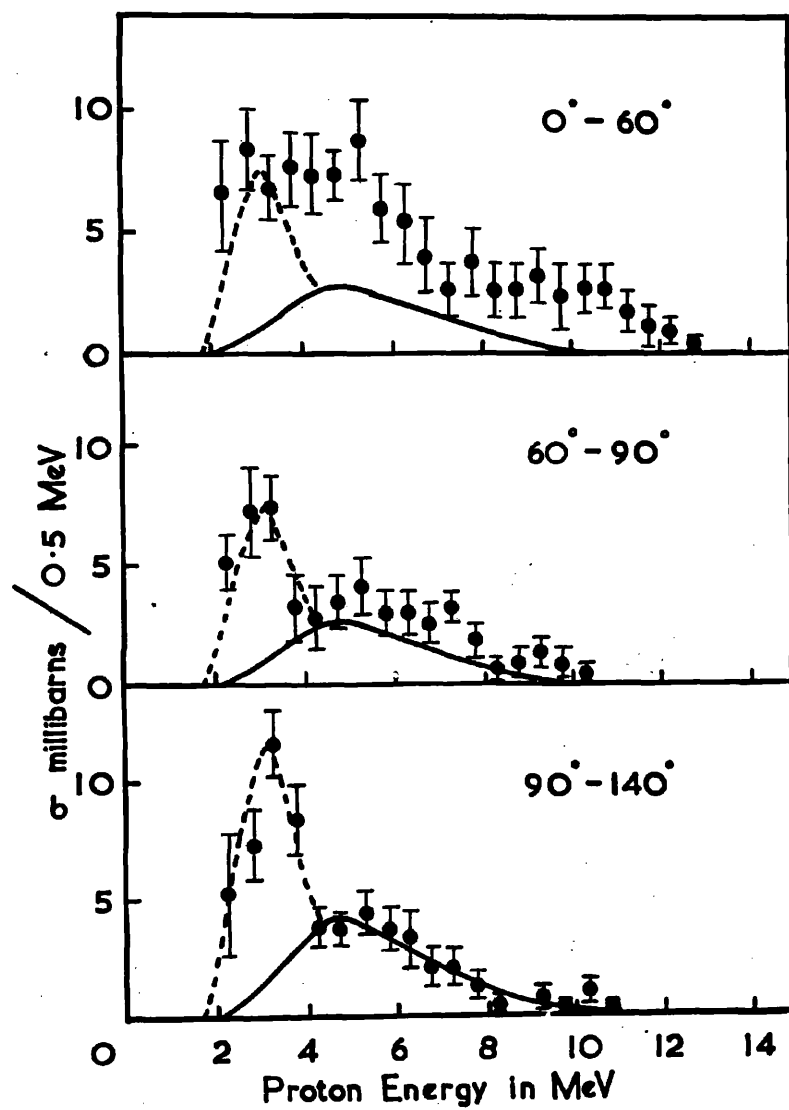


Figure 14 Energy spectrum from Ni^{60}

Weisskopf (1952) for a nucleus of radius $1.3 \times 10^{-13} A^{1/3} \text{ cm}$, where A is the mass number, were used. The results are insensitive within the experimental error to any reasonable choice of nuclear radius. The energy distribution obtained in this way was normalised to the energy distribution observed for each isotope in the angular range 90° - 140° . By assuming that protons emitted as a result of the statistical model are emitted isotropically the corresponding energy spectra were obtained for the other angular intervals taking into account the respective solid angles.

The Coulomb barrier for Fe^{54} and Fe^{56} should be almost identical and yet many more low energy protons were observed from Fe^{54} than Fe^{56} . This is presumably due to the (n, np) reaction being allowed while the $(n, 2n)$ reaction is forbidden for Fe^{54} at certain excitation energies, as discussed previously. The relevant Q values for the various processes are given in table 7.

Table 7 shows that the $(n, 2n)$ reaction cannot occur in Fe^{54} when the energy of the incident neutron is 13.5 MeV, while the (n, np) reaction is possible for proton energies from 0 to 4.3 MeV. For Fe^{56} the (n, np) reaction is only favoured with respect to the $(n, 2n)$ reaction over the energy interval 0 to 1.0 MeV where proton emission is prevented by

Table 7Q values for Fe^{54} , Fe^{56} and Ni^{60}

Isotope	Q value in MeV			Maximum energy of emitted proton (MeV)	
	(n,p)	(n,np)	(n,2n)		
				(n,np)	(n,p)
Fe^{54}	+0.34	-9.2	-13.8	4.3	13.9
Fe^{56}	-2.93	-10.2	-11.2	3.3	10.6
Ni^{60}	-2.0	-9.6	-11.5	3.9	11.5

the Coulomb barrier. A similar argument suggests enhanced proton emission from Ni^{60} for protons of energy less than 3.9 MeV.

For the angular range 90° - 140° in Fe^{54} and Ni^{60} the large low energy peak appears to cut off satisfactorily at the expected energy for an (n,np) reaction.

The broken lines in figures 9 and 11 were drawn through the experimental points at energies less than 4 MeV in the angular range 90° - 140° . This curve was then transferred according to solid angle to the other angular ranges. The good fits obtained with the experimental points indicates that the low energy peak is isotropic as would be the case if was due to an (n,np) process.

The absence of a low energy peak in Fe^{54} cannot be related to a large negative Q value for the (n,p) process in

this isotope since a low energy peak is observed in Ni^{60} which has also a large negative Q value for the (n,p) process.

The angular distributions of the protons emitted from all isotopes are approximately flat at angles greater than 90° for all energy intervals. To illustrate any departure from isotropy at forward angles the dashed line was drawn through the mean of the experimental points at angles greater than 90° for all isotopes and all energy intervals. The protons emitted from all isotopes with energies less than 4 MeV are approximately isotropic. For proton energies between 4 and 7 MeV there is a tendency for the distribution to peak at forward angles, and for energies greater than 7 MeV there is a marked peak at angles below 60° for all cases.

For all isotopes, as shown in figures 12, 13 and 14 there are more high energy protons at forward angles than would be expected from the statistical model. The energy spectra of the excess protons are approximately flat. The statistical accuracy of the results is such that the presence of structure in the energy spectrum, similar to that found by Gugelot (1954) and Cohen (1957) in the inelastic scattering of protons, cannot be confirmed.

The total cross sections for the emission of protons from the separated isotopes on bombardment with neutrons with an energy of 13.5 MeV were obtained by extrapolating the

observed angular distribution to 180° . The cross sections obtained were 600 ± 60 mb for Fe^{54} , 95 ± 20 mb for Fe^{56} and 223 ± 25 mb for Ni^{60} .

If the isotropic part of the angular distribution is assumed to be due to compound nucleus processes and the forward peaking to a direct interaction, the cross sections for these processes are given in table 8. The direct interaction cross sections obtained in this way do not include any isotropic component and so may be underestimated.

Table 8

Cross sections for Fe^{54} , Fe^{56} and Ni^{60} .

Isotope	Cross sections in mb			
	Compound nucleus		Direct Interaction	Total
	(n,p)	(n,np)		
Fe^{54}	306	224	70	600
Fe^{56}	75	0	20	95
Ni^{60}	87	68	68	223

By using a similar argument to that of Chapter III the present Fe^{56} results give an activation cross section of 93 ± 20 mb, which has to be compared with the experimental values of Paul and Clarke and of Forbes of 124 ± 12 mb and 97 ± 12 mb respectively, at a neutron energy of 14 MeV.

(vii) Nuclear Temperatures

Because of the rapid increase in the number of possible excited states with mass number and excitation energy only a statistical description is possible at present for all but the lightest nuclei and lowest excitation energy. Weisskopf (1937) first introduced thermodynamic concepts in the study of nuclear reactions. The extent to which high energy states of a nucleus are occupied is suitably expressed in terms of the temperature (T) of the nucleus. The usual expression for the energy spectra in statistical model theory is then $N(E_p) = K \sigma_{cp} E_p e^{-E/T}$ where $N(E_p)$ is the number of protons observed with an energy of E_p and σ_c is the cross section for the formation of a compound nucleus.

Since nuclear temperature is a statistical model concept it is essential to use for its computation energy spectra which contain the minimum number of protons from the result of direct interaction. Hence the nuclear temperatures for Fe^{54} , Fe^{56} and Ni^{60} were obtained using only protons in the angular range 90° - 140° .

The temperature graphs for Fe^{54} , Fe^{56} and Ni^{60} are shown in figures 15 and 16. In these $\log \left[\frac{N(E_p)}{\sigma_c E_p} \right]$ was plotted against E_p and the temperature is given by the gradient of

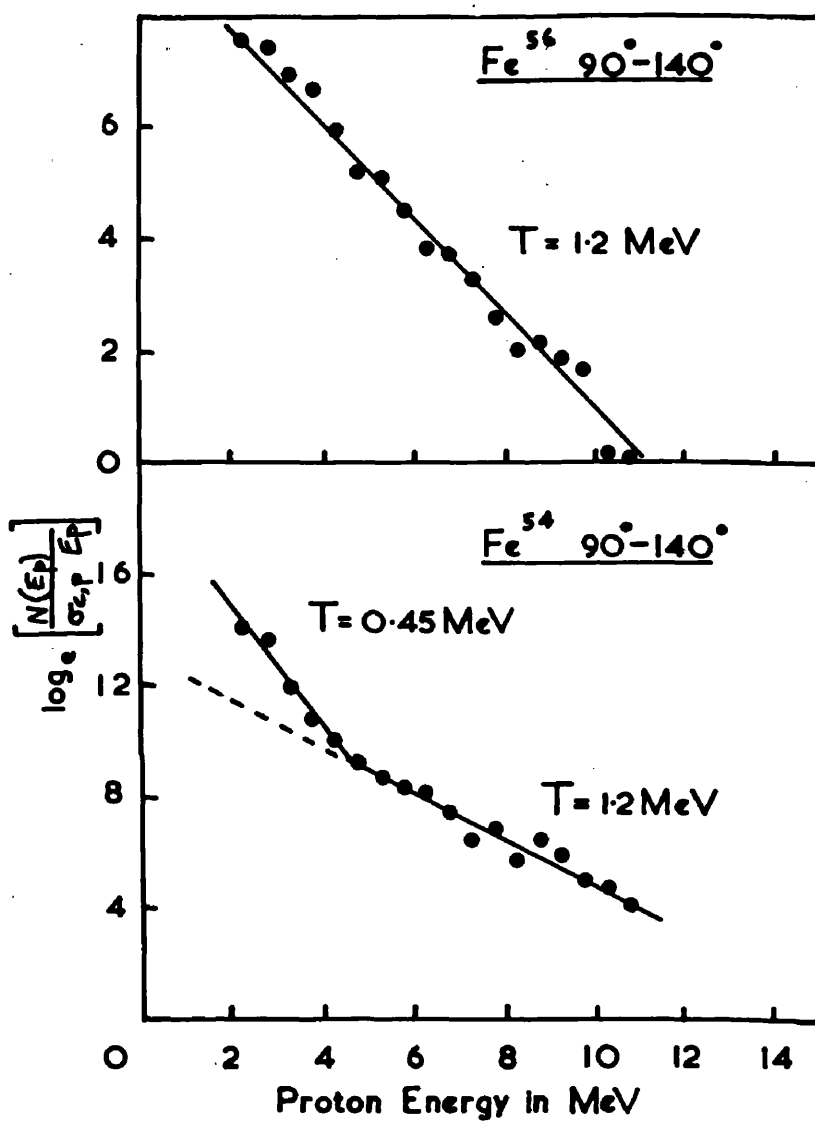


Figure 15 Temperature graphs for Fe^{54} and Fe^{56}

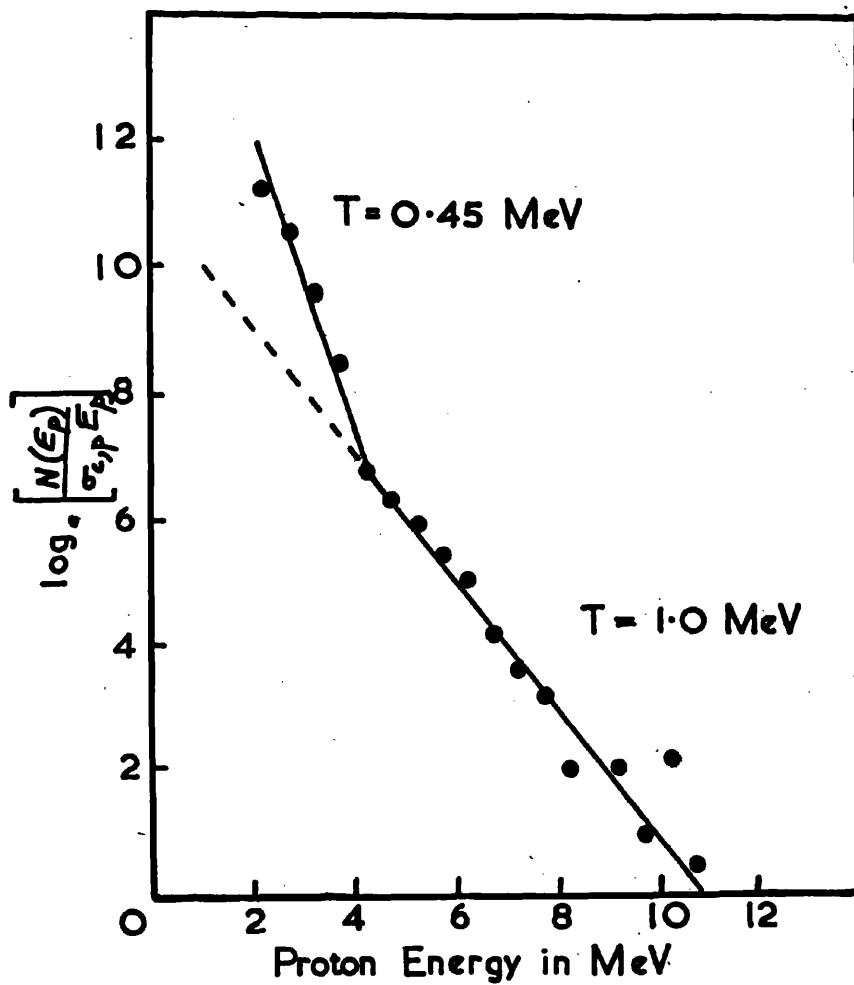


Figure 16 Temperature graph for Ni^{60}

the resulting straight line. The values of σ_{cp} used here were those given by Blatt and Weisskopf (1952) for a nucleus of radius $1.3 \times 10^{-13} A^{1/3}$ cm.

The experimental results are consistent with a straight line for Fe^{56} and two straight lines for Fe^{54} . The high energy straight line portion for Fe^{54} has the same gradient as the straight line representing all energies for Fe^{56} . This gradient corresponds to a nuclear temperature of 1.2 MeV. The junction of the straight lines in the Fe^{54} temperature plot occurs at the same energy as the onset of the (n,np) process and may be taken as illustrating its occurrence. The value of 0.45 ~~0.2~~ MeV for this process is consistent with the values obtained by Cranberg and Levin (1956) for nuclear temperatures at a few MeV excitation. This gives more weight to the interpretation of the low energy peak as due to (n,np) rather than (n,d). The Ni^{60} results on a temperature plot are very similar to the Fe^{54} results.

Nuclear temperatures have been measured for iron and nickel by various workers. Details of their results are given in table 9.

Although the efficiency for detecting neutrons by all techniques is much less than the efficiency for detecting protons, because of the Coulomb barrier it might be expected that proton emission would have a larger percentage direct

Table 9

Nuclear temperatures

Isotope	Reaction Studied	Observer	Bombarding Energy (MeV)	ΔE (MeV)	T (MeV)
Natural Iron	(n,n')	(a)	14	1-4	0.76
Natural Iron	(n,n')	(b)	15	1-3	0.6
Natural Iron	(p,p')	(c)	18	5-8 10-16	1.36 2.6
Natural Iron	(p,n)	(d)	10	2-6 5-8	0.95 1.2
Fe ⁵⁴	(n,p)	(e)	13.5	4-10 2-4	1.2 0.45
Fe ⁵⁶	(n,p)	(e)	13.5	2-10	1.2
Natural Nickel	(p,p')	(c)	18	5-8 10-16	1.2 2.6
Ni ⁶⁰	(n,p)	(e)	13.5	4-10 2-4	1.0 0.45

 ΔE Energy range over which T was measured

(a) Graves and Rosen (1953)

(d) Gugelot (1951)

(b) Whitmore and Dennis (1951)

(e) Present results

(c) Gugelot (1954)

component and so is perhaps less reliable for determining temperatures. Direct effects not subtracted would give rise to high values of the nuclear temperature.

(viii) Comparison of Results with Other Workers

During the course of the present work results on the energy spectra at forward angles of protons emitted from similar elements to those investigated here were reported by Allan (1957) using nuclear emulsions and Colli et al. (1956,1957) using a counter technique. Neither of these authors measured the angular distribution or prove satisfactorily that structure was present in the energy spectra.

Allan attempted to allocate cross sections to (n,p) and (n,np) compound nucleus and direct interaction from his energy spectra at angles $34^{\circ} \pm 20^{\circ}$. His results and the present results are given in table 10. The cross sections given for the (n,np) process are always in good agreement. Because of Allan's angle of observation it might be expected that his (n,p) compound nucleus would be overestimated and direct interaction underestimated. This appears to be the case for all isotopes except Fe^{56} . Allan's results for Fe^{56} seem to contain events above the largest energy expected from the Q value of the reaction. Figure 17 shows the results of Colli et al. (1957) for protons emitted from natural iron

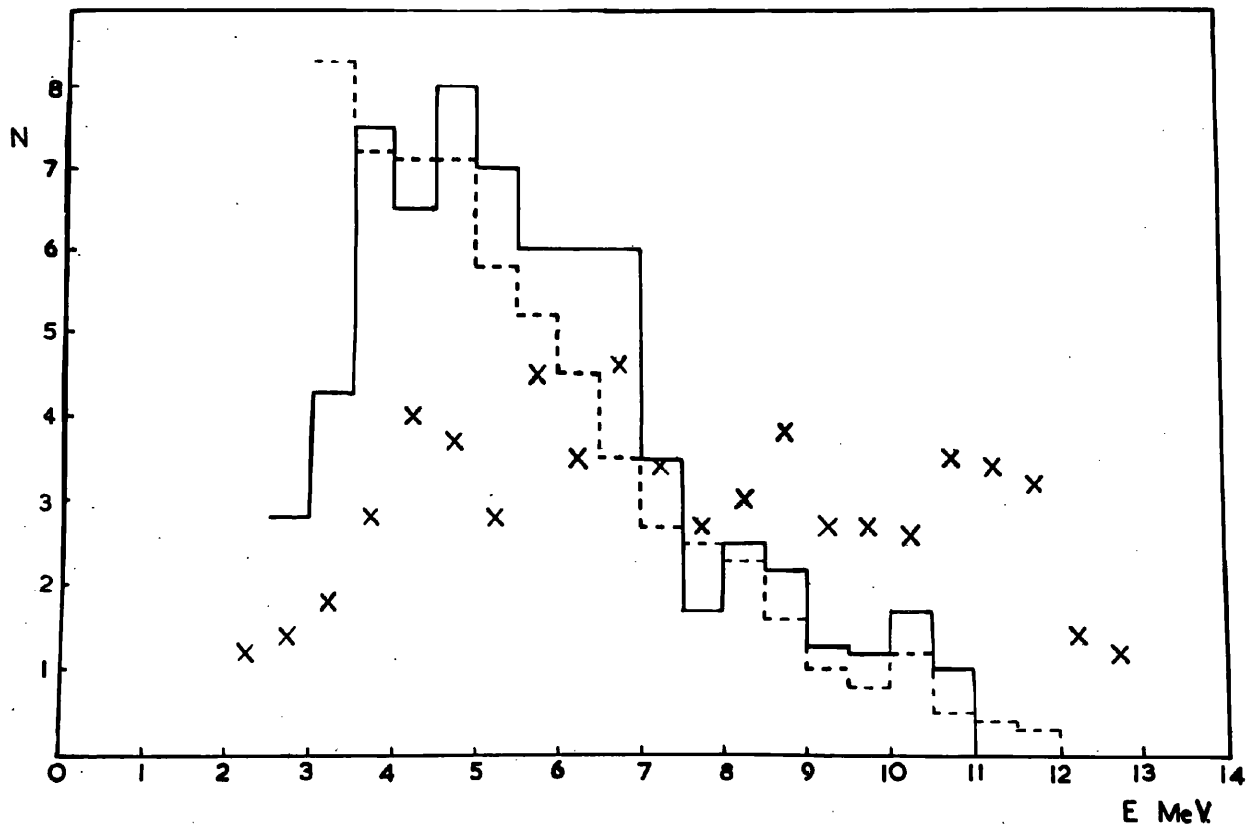


Figure 17 Energy spectra at forward angles from Fe^{56}

Solid line, present results

Dotted line, results of Colli et al. (1957)

Crosses, results of Allan (1957)

Table 10

Present results/Allan's results in mb

	Fe ⁵⁴	Fe ⁵⁶	Ni ⁶⁰
Total	600/680	95/190	223/300
(n,np)	224/220	0/0	68/60
(n,p) compound	306/460	75/100	87/200
Direct	70/0	20/90	68/40

(92% Fe⁵⁶) on bombardment with neutrons with an energy of 14.5 MeV, the results of Allan for Fe⁵⁶ separated isotope for neutrons with an energy of 14.0 MeV and the present results all measured at forward angles and normalised to the same cross section. The large number of high energy tracks reported by Allan suggests an incorrect background subtraction

Recently results have been presented by Colli et al. (1958) for calcium using counters and Allan (1958) for copper using nuclear emulsions on the angular distribution of protons emitted on bombardment with neutrons with an energy of the order of 14 MeV. Both groups deduce conclusions similar to those given here concerning forward peaking of the angular distribution. Allan claims to have found structure in his energy spectrum.

Work of a similar nature is at present being performed in a number of laboratories among them the Glasgow H.T. set.

(ix) Comparison With Direct Interaction Theories

The cross sections obtained experimentally for Fe^{54} , Fe^{56} and Ni^{60} were 600 mb, 95 mb and 223mb while the theory of Brown and Muirhead gives 595 mb, 100 mb and 130 mb respectively. The energy spectra observed experimentally indicates more low energy protons from Fe^{54} and Ni^{60} than this theory would predict. An explanation of this discrepancy as due to an (n,np) process has been discussed above and hence the agreement of the experimental cross section with theory for Fe^{54} may be fortuitous.

According to the theory of Brown and Muirhead the more negative the Q value for the process the larger will be the ratio of direct to compound cross section. For the isotopes investigated here the ratio of direct to (n,p) compound cross section is 0.23, 0.27 and 0.77 while their theory predicts 0.1, 0.37 and 0.26 for Fe^{54} , Fe^{56} and Ni^{60} respectively. Thus the variation predicted with Q value for different isotopes was not observed.

A doubtful assumption in this theory is in the calculation of Coulomb penetrabilities for protons in which they used the ratio of the cross section for the formation of a compound nucleus by protons and neutrons. The distribution of angles at which a particle leaves a nucleus will in general be different from the angles at which it enters.

The angular distribution of the protons emitted from Fe^{54} has been compared with the predictions of two theories (figure 18). Since most of the protons arising in direct interaction would be expected to be of high energy comparison has only been made for protons of energy greater than 7 MeV. Elton and Gomes (1957) while considering the inelastic scattering of protons with an energy of 31 MeV from tin traced the paths of individual nucleons through the nucleus and found that total internal reflection reduced to negligible amounts direct effects arising in the nuclear volume. This treatment of surface direct interaction is not immediately transferable to lower energies. The criterion here is that the reduced wavelength at the height of the Coulomb barrier is less than, or approximately equal to, the surface thickness ($\sim 1.5 \times 10^{-13}$ cm). This corresponds to an incident energy of at least 10 MeV above the Coulomb barrier and so the present investigation is on the limit of validity of this theory. To fit the angular distribution of protons with energy greater than 7 MeV it was assumed that the entire cross section was due to surface direct effects. It was then necessary to assume three effective protons for scattering per nucleus. That is of the order of nine protons per nucleus are required to be outside the Coulomb barrier.

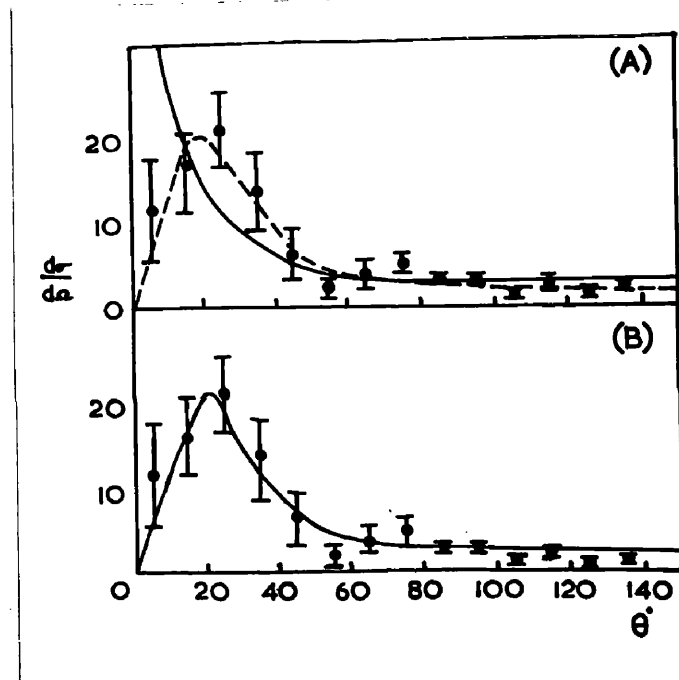


Figure 18 Differential cross section ($\frac{d\sigma}{d\Omega}$) in mb/ster.
for Fe^{54}

- (A) Solid line theory of Brown and Muirhead (1957)
Dotted line theory of Elton and Gomes (1957)
- (B) Solid line volume direct interaction with
angular momentum conserved

(x) A Modification To The Theory of Brown and Muirhead

The Fe^{54} experimental results appear to place some doubt on the direct interaction taking place entirely at the nuclear surface. Apart from the unsatisfactory nature of the Coulomb penetrability in the model of Brown and Muirhead, a difficulty which cannot easily be surmounted, the other serious omission in this theory is the neglect of the conservation of angular momentum.

The argument presented here is similar to that usually applied to surface direct interaction (Butler 1957). This method of approach is entirely classical. Let a nucleon, assumed to be at rest, at a distance r_1 from the centre of a nucleus be struck by a projectile having a momentum p_i . Let the final momentum of the outgoing particle be p_f . If the momentum transfer to the nucleus is $\hbar Q$, then

$$\hbar Q = p_i - p_f$$

Thus the angular momentum transferred to the nucleus is

$$|M| = \hbar |Q \wedge r_1| = \hbar Q r_1 |\sin \beta|$$

where β is the angle between Q and r_1 . Now the angular

momentum given to the nucleus can only be integral multiples of \hbar and so $e = Q r_1 |\sin \beta|$

$$\text{or } \sin^2 \beta = \frac{e^2 \hbar^2}{r_1^2 (p_i^2 + p_f^2 - 2 p_i p_f \cos \theta)} \quad (6)$$

where θ is the angle between p_i and p_f .

The nucleus can then be considered as divided into shells of constant radius r_1 and the number of nucleons in

each shell calculated assuming a constant nuclear density. The number of effective nucleons in each shell for emission of a particle with a given angle and energy can now be calculated using equation 6.

The angle and energy distribution of nucleons without taking into account the conservation of angular momentum was calculated using the equations of Brown and Muirhead for the collision of a neutron with an energy of the order of 14 MeV with a Fermi gas of nucleons. These equations take into account the Pauli exclusion principle and the Q value of the reaction. To the distribution of emitted particles according to angle and energy was applied the factor determined above for the number of collisions within the nucleus which could satisfy angular momentum conservation. The resulting angular distribution is shown, compared with the Fe^{54} experimental results, in figure 18. Because of uncertainties in Coulomb penetrability the theoretical curve was normalised to the experimental points. The normalising factor was ~ 2 . The absolute theoretical cross section for direct interaction is equal to the cross section for direct interaction within the nucleus multiplied by a factor (~ 0.2) determined by the Coulomb penetrability and the mean free path of a nucleon in nuclear matter. Hence the present experiments indicate that the latter factor has been underestimated probably due to enhanced emission at the

nuclear surface.

The most significant difference in the angular distribution resulting from the inclusion of angular momentum conservation is the disappearance of the very high peak at angles less than 5° . None of the experimental angular distributions gave evidence for such a peak.

The shape of the energy spectra is altered very little by including angular momentum conservation.

Conclusions

The protons emitted from Fe^{54} , Fe^{56} and Ni^{60} appear to result in part from a direct nucleon-nucleon collision. It is possible to explain the results qualitatively by a model assuming nucleon-nucleon collisions within complex nuclei, with a possible enhanced emission at the nuclear surface, and including angular momentum conservation. Any subsequent de-excitation of the nucleus is by compound nucleus decay.

The low energy protons from the isotopes investigated in this Chapter appear to arise from an (n, np) reaction when the $(n, 2n)$ reaction is energetically unfavourable.

CHAPTER V

COLLIMATED NEUTRON BEAM STUDY OF ALUMINIUM

(i) Introduction

To investigate more fully the energy spectra of charged particles emitted as a result of neutron interactions in the 14 MeV energy range a new experimental arrangement has been designed and constructed. This was made possible by the higher neutron fluxes available.

The disadvantages of the previous arrangement are two fold. Since the nuclear emulsions are not shielded from the neutron source there always exists a large background subtraction due to knock-on protons and other optically unresolvable events inside the emulsion. These considerations suggest that a collimated neutron beam should be used. The other main disadvantage is the limited energy resolution due to the long distances protons travel through the foil of the material being investigated. This disadvantage has its origin in the thickness of the foil and the acceptance angles of tracks in the photographic emulsion which can be detected with high efficiency. The difficulty in observing steep tracks made it impossible to detect with high efficiency tracks

passing through the foil at angles greater than 45° in the previous arrangement. In order that tracks of greater dip may be observed it is necessary to incline the surface of the emulsion to the surface of the foil. This involves the separation of the emulsion from the foil and so the introduction of an additional solid angle. The magnitude of this solid angle will be principally determined, if a collimated beam is used, by the dimensions and type of collimation.

It is not possible to use a scattering foil of large area without introducing corrections to the incident neutron direction and also additional background due to protons from the foil but outwith the efficient range of observation.

The interpretation of the low energy peak found in the previous aluminium exposures (Chapter III) was not altogether clear. The angular distribution of protons with an energy less than 4 MeV suggested that these protons might be forward peaked. Hence it was decided to investigate the charged particles emitted from aluminium.

Shortly after the start of this experiment results were reported by Haling et al. (1957) for the charged particles emitted from aluminium on bombardment with

neutrons with an energy of 14.0 MeV using nuclear emulsions and a collimated neutron beam. They obtained a forward peaking of the low energy protons. Their results suggested that the low energy peak moved towards higher energy with increase of angle to the incident neutron direction. An effect of this type was not found for any of the isotopes previously investigated here. The results of Haling et al. did not allow a detailed comparison of the energy spectrum at forward and backward angles. It was decided to investigate this.

The results of Allan (1957) suggested that the low energy peak at forward angles in aluminium might consist of two peaks.

(ii) Apparatus and Exposure

The apparatus which is shown schematically in figure 19 consists essentially of two parts; a collimator and a scattering camera. By considering the cross section for neutron interactions and the number of scattering centres per unit length an iron collimator was chosen in preference to lead. The collimating properties of brass are as good as those of iron.

In the design of the apparatus the reduction in

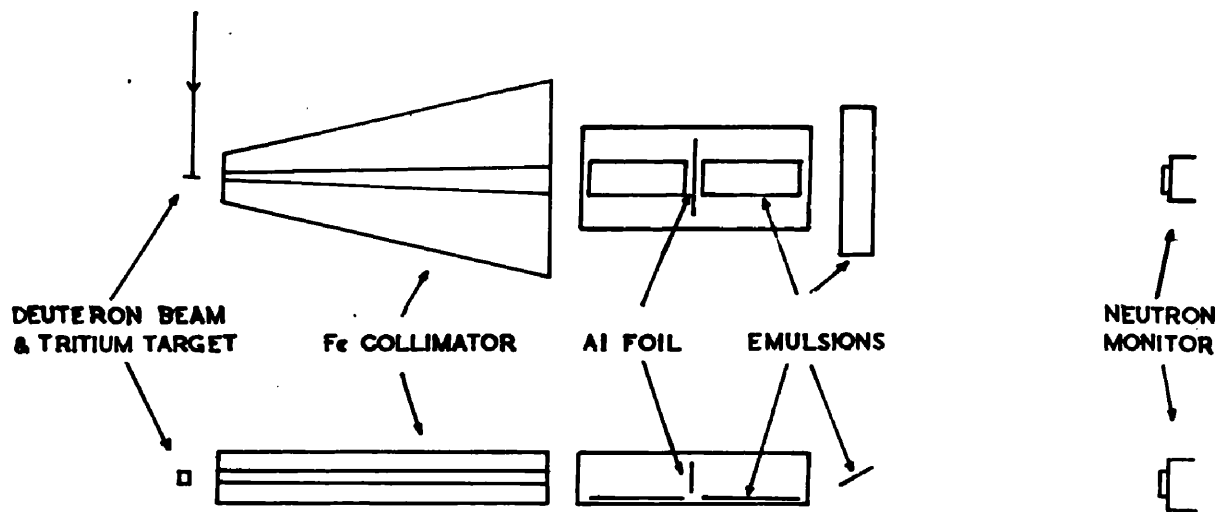


Figure 19 Schematic diagram of apparatus

neutron intensity at an emulsion placed within the scattering camera was considered as a function of the two solid angles involved for the detection of protons from a foil placed at the centre of the scattering camera. The solid angles considered were those subtended at the foil by the tritium target and the solid angle subtended at the emulsion surface by the foil. The length of the scattering camera was determined by the angular range of protons which might usefully be investigated. The optimum conditions were found to be a collimator of length 10" (that is of the order of four mean free paths in iron for neutrons with an energy of 14 MeV) and a scattering camera of length $6\frac{1}{2}$ ". The scattering camera was an evacuated box $6\frac{1}{2}" \times 2\frac{3}{4}" \times 1\frac{1}{4}"$ of brass $1/16"$ thick.

The dimensions of the collimator were such as to shield the camera from the neutron source. The height of the collimator was $1\frac{1}{2}"$ and the breadth at the camera end was 6". The breadth at the end next to the neutron source was $1\frac{1}{2}"$.

A cylindrical hole of radius $\frac{1}{2}"$ was cut out of the centre of the iron collimator. A brass pipe was made to fit exactly into this hole. This allowed variations in the shape and size of the collimating slit without requiring a

new collimator for each case. The brass pipe ^{used for} ~~in~~ the exposure ~~scanned~~ had a tapered rectangular hole. The dimensions of the cross section of this slit at the front end of the collimator was 1.2 cm x 1 cm and at the other end 2 cm x 1 cm. These dimensions were calculated using the nearest distance that the iron collimator could be placed to the neutron source. The object of the tapered hole was to eliminate, as much as possible, neutrons from being degraded in energy by passing through only part of the iron (or brass) collimating system.

The foil to be investigated was stretched across the centre of the camera perpendicular to the direction of the neutron beam. The emulsions were placed on the floor of the box with their long sides parallel to the neutron beam direction. All parts of the interior of the box (that is all parts except the floor) from which protons could reach the emulsion surface and appear to come from the foil were covered by 400 micron thick sheets of fine gold.

The collimator and camera were held in position on a common base to prevent relative changes in their position during the exposure.

An aluminium foil of thickness 14 mg/cm^2 , placed in position in the scattering camera, was exposed to

neutrons from the $T(d,n)He^4$ reaction induced by deuterons accelerated on the 200 KeV Glasgow H.T. set. The set was operated during these exposures at an energy of 150 KeV. The line of the collimating slit was at right angles to the deuteron beam direction, and so the neutrons considered had an energy of 14.1 ± 0.1 MeV (Fowler and Brolley, 1956). The end of the collimator was 5 cm from the neutron source. The tritium zirconium target was mounted at right angles to the deuteron beam direction, and hence presented a line source with respect to the collimating slit direction.

The neutron flux was monitored throughout the exposure by a plastic scintillation counter frequently calibrated by the aid of a kicksorter.

The integrated neutron flux was checked by means of nuclear emulsions. A nuclear emulsion was placed across the neutron beam at the far end of the brass box. The emulsion surface was at an angle of 30° to the incident neutron direction. A 400 micron thick sheet of gold was placed on top of the emulsion to shield it from external sources of protons. This nuclear emulsion was changed halfway through the exposure.

The emulsions were processed by the method described previously.

(iii) Neutron Flux Measurements and Efficiency of Collimator

On developing the flux monitor emulsions a black band was clearly observable with the unaided eye across the centre of the emulsion suggesting a high efficiency of collimation.

A known volume of the flux monitor emulsion was scanned for knock-on protons by the procedure previously described (Chapter IV). Although the neutron flux was higher than in the previous exposures in which volume scanning was carried out the efficiency for detecting the start of proton tracks was of the order of 95%. Fields of view at regularly spaced intervals were examined across the width of the emulsion exposed to neutrons which had passed down the collimating channel. No significant fluctuation in neutron intensity across this area was observed.

The energy and angle with respect to the incident neutron direction was calculated for all tracks. The tracks resulting from the collision of a neutron with an energy of 14.1 MeV with the hydrogen of the emulsion was obtained in the usual way by considering the accuracy of measurements.

Since the geometry of the flux plates was the same as that used in Chapters III and IV the geometrical efficiency factors used there (figure 3) were again used.

The distribution of knock-on protons was found to be isotropic within the experimental errors. The integrated neutron flux at the monitor emulsion surfaces was found to be 5.7×10^8 neutrons/cm² and 7.2×10^8 neutrons/cm². The ratio of the neutron intensity at the two emulsions as given by the plastic scintillator was 1.5.

A volume of emulsion within the camera was searched for tracks starting and ending within the emulsion. Tracks of projected length greater than $22\frac{1}{2}$ microns at all horizontal angles with dips less than 50° to the unprocessed emulsion surface were measured in the usual way. By considering the total dip of the track and the thickness of the emulsion a factor was obtained to allow for the layer at the top or bottom of the emulsion in which a track originating of the total dip being considered would not have terminated in the emulsion. The second stage of the correction allowed for the dip cut-off at 50° to the unprocessed emulsion surface. For a track at an angle θ to the incident neutron direction the correction factor was

$$\frac{2}{\pi} \sin^{-1} \left(\frac{\sin 50^\circ}{\sin \theta} \right)$$

The number (R) of knock-on protons found in the emulsion exposed in the camera divided by the number which would have been found without neutron collimation for

various knock-on proton energies is given in table 11.

Table 11

Efficiency of collimator

	Knock-on Energy in MeV		
	2-4	4-7	7-14
R	0.26	0.16	0.12

(iv) Scanning Procedure and Analysis of Data

The emulsion surfaces of plates exposed in the camera were scanned in a region corresponding to protons from the aluminium foil in the angular range 16° - 48° and 132° - 164° by the procedure outlined in Chapter 1V for tracks crossing the emulsion surface. Only tracks compatible with the assumption that the particle originated at the aluminium foil were accepted. This condition implied that only tracks with dip between 5° and 50° to the unprocessed emulsion surface and horizontal projected angle of 0° to 50° on the emulsion surface with respect to the incident neutron direction were measured. No tracks with a projected length on the emulsion surface less than $22\frac{1}{2}$ microns were measured.

The energy of all accepted tracks was obtained, as previously, by assuming that they were protons and

applying the range energy tables of Rotblat (1951). The angle of all such tracks was also found with respect to the incident neutron direction.

The background subtraction for forward angle tracks was obtained by scanning the emulsion on the other side of the aluminium foil in a symmetrically opposite position for tracks satisfying the same geometrical conditions. The background for backward angle tracks was obtained in the same way. This method is valid since the areas scanned were close to and symmetrical about the centre of the scattering camera and far from the ends where the neutron beam enters and leaves where most of the local background might be expected. The number of tracks found in the various areas is given in table 12.

Table 12

	Forward Angles (16° - 48°)	Backward Angles (132° - 164°)
Area scanned	0.513 cm ²	0.441 cm ²
Tracks accepted	2123	741
Background tracks	307	118
Tracks from Al	1816	623

As illustrated in table 12, the neutron collimator and the thicker radiating foil, made possible due to shorter path differences in the foil of the particles investigated, greatly reduced the percentage of background tracks as compared to the apparatus used in the investigations described in Chapters III and IV.

A correction was applied for the loss of energy of tracks passing through the aluminium foil by adding to each track the energy a proton would have lost in penetrating half the thickness of the foil. Thus protons having ranges in the emulsion corresponding to energies of 2, 6 and 10 MeV were considered to have had initial energies of 2.75 ± 0.75 , 6.4 ± 0.4 and 10.2 ± 0.2 MeV, respectively.

The number of tracks observed at each angle was corrected for the geometry of the apparatus. This was performed using the geometrical efficiency factors obtained by the method described in Appendix 1.

A small correction to the low energy tracks was applied since no tracks with projected length on the emulsion surface less than $22\frac{1}{2}$ microns were accepted.

(v) Energy and Angular Distributions

Figure 20 shows the energy spectra of charged

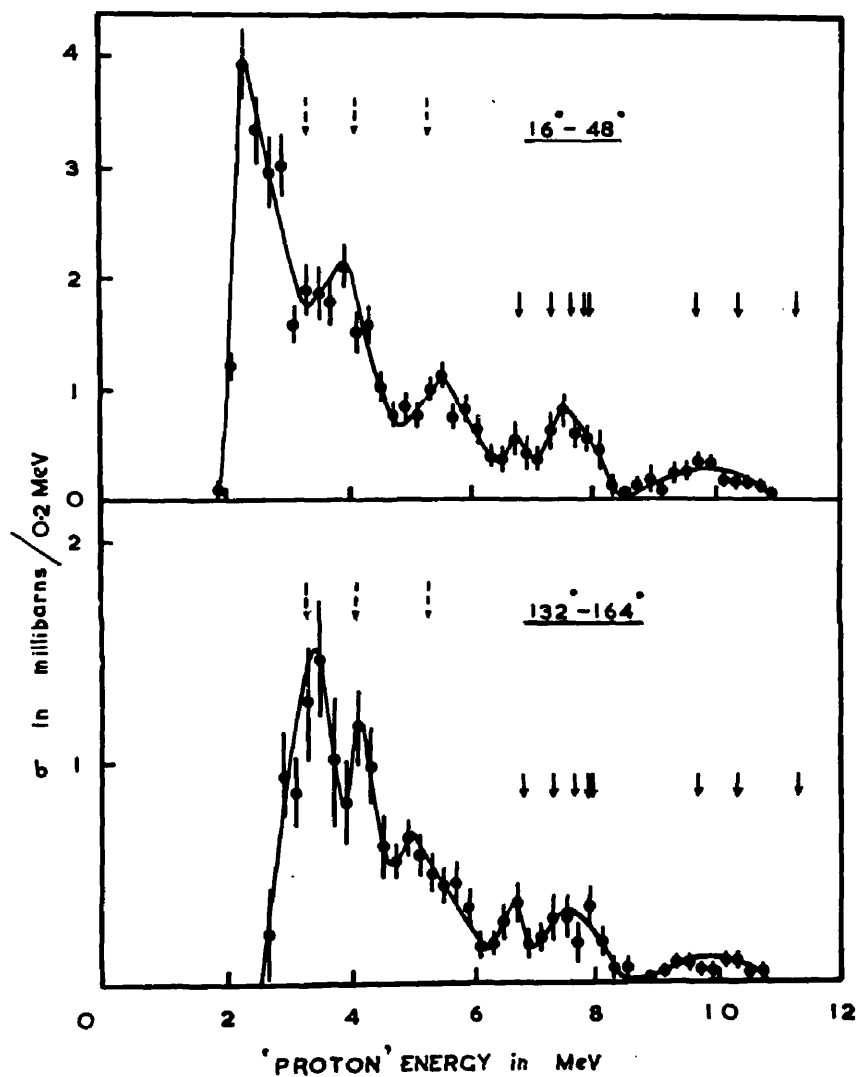


Figure 20 Energy spectra from aluminium

particles emitted from aluminium on bombardment with neutrons with an energy of 14.1 MeV for the angular ranges 16° - 48° and 132° - 164° . The proton energies shown in this figure are centre of mass energies. The energy spectra at forward and backward angles exhibit structure. The solid arrows correspond to the energy levels observed in the deuteron stripping reaction $\text{Mg}^{26}(\text{d},\text{p})\text{Mg}^{27}$ as reported by Hinds et al. (1958). This reaction is dependant on the energy levels in the Mg^{27} nucleus, which is the residual nucleus in an (n,p) reaction in Al^{27} . The levels as observed by Hinds et al. are at energies of zero, 1.0, 1.66, 3.50, 3.56, 3.75, 4.13 and 4.75 MeV. The ground state (n,p) transition was not observed. Not all of the other levels have been resolved. There exists a broad group at proton energies of about 10 MeV corresponding to the 1.0 and 1.66 MeV levels, and another broad group at a proton energy of 7.5 MeV corresponding to the levels at 3.50, 3.56, 3.75 and 4.13 MeV. The 4.75 MeV level has been resolved as is shown most clearly in the backward angle energy spectrum.

Since it is not possible to distinguish protons and deuterons in Ilford C.2. nuclear research emulsions the energy spectra displayed may contain deuterons. The

maximum possible deuteron energy as determined by the Q value for the (n,d) process is 6.9 MeV. Since the energy spectra shown here were assumed to contain only protons any deuterons present would be assigned the wrong energy. Table 13 shows the energy of deuterons with the same range as protons of a fixed energy. This table shows that no deuterons can be present in the energy spectra at energies above '5.3 MeV'.

Table 13

Energy of deuteron with same range as proton of given energy

Proton energy	5.3	4.3	3.3	2.3
Deuteron energy	6.9	5.6	4.2	2.9

A small error will also be introduced because of the assumption that all particles were protons when correction was made for the energy loss in the aluminium foil and in the centre of mass transformation.

An (n,d) reaction in Al^{27} will involve the energy levels of Mg^{26} . Levels in this nucleus were reported at 1.8 and 3.0 MeV by Endt and Kluyver (1954). These together with the ground state transition are indicated by dotted arrows in figure 22.

If the low energy particles displayed in figure 22

were in fact deuterons use of the proton energy correction and centre of mass motion would each displace the low energy tracks by about 0.3 MeV. Thus at forward angles the spectrum would be displaced by about 0.6 MeV towards lower energies while at backward angles the displacements would cancel. Hence the low energy peaks in the energy spectra are consistent with the reaction $\text{Al}^{27}(\text{n},\text{d})\text{Mg}^{26}$ indicating that a large portion of these tracks are deuterons.

Absolute cross sections were obtained using the monitor emulsions exposed directly to the collimated neutron beam.

The distribution in angle of the protons observed at forward and backward angles are shown in table 14. These results indicate a smooth variation of the number of protons with angle over the angular range investigated. Many more protons were found at forward than backward angles for all energy intervals. The ratio of forward to backward cross section is given in table 15. In the classification given in this table the majority of the low energy tracks were assumed to be deuterons.

The forward peaking of the low energy protons (less than 4 MeV) shows that a direct mechanism such as (n,d) must be responsible for most of the particles as

Table 14

Cross section in mb/ster

Energy	Angular interval							
Interval (MeV)	16-20	20-24	24-28	28-32	32-36	36-40	40-44	44-48
< 4.0	21.6	14.0	10.5	10.0	10.0	9.4	9.6	8.7
> 4.0	9.6	7.9	7.2	9.1	6.3	6.1	7.7	7.2

Angular	132-	136-	140-	144-	148-	152-	156-	160
interval	136	140	144	148	152	156	160	164
all energies	8.2	6.6	6.8	7.2	8.0	7.4	6.8	8.2

Table 15

Forward to backward ratio

Proton	2.0-	3.8-	5.0-	6.4-	8.6	Total
energy MeV	3.8	5.0	6.4	8.6		
	2.8	2.8	2.1	2.1	3.5	2.63

opposed to an (n,np) reaction.

The ratio of the differential cross section for all particles emitted in the forward angular interval to that for the backward interval is 2.63 in good agreement with the value of 2.69 obtained by Haling et al. (loc. cit.) for the ratio of the differential cross section at $30^{\circ} \pm 15^{\circ}$ to that at $150^{\circ} \pm 15^{\circ}$. The absolute value obtained here for the differential cross section in the forward interval

is 19.3 mb/ster. while Haling et al. obtained 9.8 mb/ster. at $30^{+15}_0^\circ$.

If it is assumed that the angular distribution of particles emitted at angles greater than 90° is flat and that the distribution between 48° and 90° is smooth then the total cross section for single charged particle emission from aluminium is 117 mb. The result obtained in Chapter III was 140^{+30}_0 mb.

Conclusions

The peaks observed in the energy spectra of charged particles emitted from aluminium are in agreement at forward and backward angles with the levels expected from previously studied reactions involving the same residual nuclei. Forward peaking was found for all energies of emitted particles. The particles observed at low energies are probably deuterons.

CHAPTER VI

960 MeV NEUTRON INDUCED REACTIONS

(i) Introduction

In general high energy nuclear reactions produced by neutrons have been studied less than the corresponding proton reactions. The fundamental neutron reaction is its mode of interaction with a proton or another neutron. To study the n-p interaction it is possible to bombard deuterons with protons. This method is rather unsatisfactory chiefly because of the shadow effect of the proton on the neutron of the deuterium nucleus. These considerations together with the impossibility of studying the n-n reaction with a proton beam make it desirable to have a source of high energy neutrons. Such neutrons may be obtained in two ways. Deuterons may be accelerated and neutrons obtained from a stripping reaction. The alternative possibility is to accelerate protons and produce neutrons in a charge exchange scattering using a beryllium or some such nucleus as a target.

The neutrons obtained from these sources are of course not monoenergetic. It would be hoped that the

neutron spectrum would contain many neutrons with an energy comparable to that of the accelerated proton. However, many low energy neutrons might also be expected from the decay of compound nuclei. For visual techniques in which, in general, particles of all energy are recorded it is essential to have an estimate of the contamination of the neutron beam with low energy neutrons.

At high energy the disintegration of complex nuclei is pictured as taking place by the Goldberger model as described in Chapter I. That is by considering individual nucleon-nucleon collisions within the nucleus. At these energies it would be expected, partly due to exchange scattering, that disintegrations produced by a neutron or a proton in complex nuclei would have similar characteristics. The characteristics of the disintegration of the nuclei of a nuclear research emulsion by high energy protons have been studied by a number of workers. Lock and March (1955) and Lock et al. (1955 a,b) used protons with an energy of 600 MeV and 950 MeV respectively, Philbert (1956) used 900 MeV protons, and Lanutte et al. (1955) used 2,300 MeV incident protons. Many more studies have been performed at lower energies, but these will be neglected since meson production would not play an

important part. No similar studies have been made with neutrons with an energy above about 350 MeV (Bernardini et al. 1952a). Hence it was decided to check the assumptions that high energy nuclear disintegrations produced by neutrons and protons are similar, and, at the same time, to use this assumption, if it was found to be valid to obtain an estimate of the number of high energy neutrons in the beam. Since it was not possible to monitor the neutron beam during the exposure a study of the interactions with complex nuclei would serve as a monitor by comparison with known cross sections.

(ii) Neutron Source and Exposure Conditions

The circulating proton beam of the Birmingham proton synchrotron working at an energy of 960 MeV was allowed to strike a 3" thick Be target placed within the wall of the chamber. The nuclear emulsions were placed in a collimated neutron beam at a distance of 10 metres from the Be target. Protons were bent away from the emulsions by the fringing field of the machine. The emulsions were exposed with their surface horizontal and one edge parallel to the neutron beam direction.

In the first exposure Ilford G.5. emulsions on

glass backings were used. In later work to allow a longer path length of track to be followed pellicles of G.5. and L series emulsions were used. The usual developing procedure was adopted.

A. Complex Nuclei Events

(i) Scanning Procedure

The emulsions were searched for two or more tracks appearing to originate at the same point. A Watson binocular microscope with a x20 oil immersion objective and x10 eyepieces was employed. A volume of emulsion of $1.19 \times 10^{-2} \text{ cm}^3$ was scanned and 278 events found.

All events were examined using a x90 oil immersion objective to confirm that the tracks did actually originate at the same point. The projected angle and dip of all tracks was measured and all tracks were followed until they left the emulsion or stopped. The range of all tracks which ended in the emulsion was measured. The grain density in a projected length of 150 microns was measured using a x90 objective of tracks leaving the emulsion.

Tracks ending in the emulsion were classified as to whether they were due to singly or doubly charged particles. All singly charged particles will be referred

to as protons, doubly charged particles as alpha particles.

The emulsions were searched for γ - μ -e decays in which the electron remained within the emulsion for more than 300 microns. Such an electron being relativistic provided a normalising point to grain density measurements.

(ii) Analysis of Events

The angle of the prongs of all stars was obtained with respect to the incident neutron direction. The energy of prongs stopping within the emulsion was obtained from range energy tables. The energy of tracks passing out of the emulsion was obtained from their grain density. The tables used for singly charged particles were those for protons and for doubly charged particles those for alpha particles.

Some charged particles which undergo a nuclear interaction in the emulsion will be confused with neutron induced stars. In particular the nuclear scattering of a proton will occur frequently and may be recorded as a two prong star. Events in which the grain densities of both prongs of a two prong star were equal were assumed to be due to the elastic scattering of protons and so eliminated from the analysis. Inelastic scattering of protons could

only be eliminated in cases where the direction of motion of the prongs could be determined.

The events were classified using the notation of Lees et al. (1953). That is an event or star having n secondary branches, (all the branches in the case of a neutron induced reaction are, of course, secondaries) of length greater than 10 microns, is denoted as an n -prong star. The limit of 10 microns was taken to eliminate recoiling nuclei.

(iii) Division of Events into Heavy and Light Nuclei

As is indicated in table 1 the constituents of a nuclear research emulsion can be divided into two groups. These are the light nuclei carbon, nitrogen and oxygen and the heavy nuclei silver and bromine. Except for hydrogen, to which kinematic considerations may be applied, the separation of events into heavy and light nuclei is not easily achieved. Because of the very low grain density of minimum ionising tracks in dilute emulsions the use of dilute emulsions is not completely satisfactory. The method usually adopted to achieve this separation is known as the alpha particle method.

The alpha particle method was first suggested by

Heidmann and Leprince-Riguet (1948). This method is based on the assumption that an alpha particle with an energy of 9 MeV or less will experience great difficulty in penetrating the Coulomb barrier of a silver or bromine nucleus. An alpha particle with an energy of 9 MeV has a range of 50 microns in a nuclear emulsion and a proton of this range has an energy of 2.3 MeV. Such a proton will also experience great difficulty in penetrating the Coulomb barrier of a heavy nucleus as is illustrated by the $\text{Rh}(n,p)\text{Ru}$ experimental results in Chapter III. The largest number of charged particles which can be emitted from a light nucleus is 8 which will arise from the complete disintegration of an oxygen nucleus. Meson effects will be neglected here. Hence any star in which there was 8 or less charges apparent and which had a track of length less than 50 microns, but greater than 10 microns was assumed to represent the disintegration of a light nucleus.

There are certain serious limitations to the alpha particle method. If a light nucleus produces a star without a prong of length between 10 and 50 microns then the above classification would not include this event as a light nucleus disintegration. In general this would be expected the smaller the number of emitted particles. If a

large portion of the excitation energy of a heavy nucleus is concentrated near the surface an alpha particle or proton at the surface may be emitted without penetrating the full Coulomb barrier. Although it would appear that the alpha particle method is suspect for a number of reasons it has been found in the past to give fair agreement in investigations where more than one method has proved feasible.

In the present investigation 44 of the 273 events, that is 15%, were assigned to reactions induced in light nuclei. This result may be compared with the results of Lock and March (loc. cit.) and Lock et al. (loc. cit.) who obtained 21% and 8% using incident protons with an energy of 600 MeV and 950 MeV respectively.

It is possible to compare these results with the absorption cross section for protons and neutrons at various energies obtained using counters. Results of experiments of this type are shown in table 16. The work at an energy of 650 MeV was performed by Moskalev and Gavrilovskii (1956), Booth et al. (1958) at 765 MeV, Chen et al. (1955) at 860 MeV, Booth et al. (1957) at 895 MeV and Coor et al. (1955) at 1400 MeV. In the case of incident neutrons the effective energy is given which they predicted from the expected

Table 16

Absorption cross section in mb

Element	Incident particle and energy (MeV)				
	650	765	860	895	1400
	protons	neutrons	protons	protons	neutrons
carbon	227	200	209	230	201
copper	850	780	728	740	671
lead	1930	1800	1680	1660	1727

Table 17

Contribution of emulsion nuclei

Element	σ_a	$N \times 10^{-22}$	$\sigma_a \times N \times 10^{-22}$
Ag	1070	1.03	1100
Br	850	1.02	866
C	230	1.36	312
N	250	0.29	72.5
O	280	1.02	285

Table 18

Prong distribution of heavy nuclei

Number of prongs	2	3	4	5	6	7	8	9
Number of stars	50	54	37	30	25	14	8	7

Number of prongs	10	11	12	13	14
Number of stars	5	1	2	-	1

shape of the neutron spectrum and the variation of the efficiency of the counter with energy.

The number of nuclei $(N)/\text{cm}^3$ of the various elements constituting a nuclear research emulsion is given in table 17. Also shown is an estimate of the absorption cross section (σ_a) for a neutron induced reaction at an energy of the order of 900 MeV as obtained from the results shown in table 16. The last column shows the product of the absorption cross section and the number of nuclei per cm^3 . Hence it follows that 25% of the interactions observed in the nuclear emulsion of the present experiment might be expected to be due to light nuclei. Since in the present experiment 15% of the interactions were found to take place in light nuclei by using the alpha particle method, perhaps not all of the light nuclei events have been discovered. A defect in the method is not unexpected. However, the alpha particle method does allow a reasonable separation into heavy and light nuclei.

(iv) Prong Distribution

The prong distribution for heavy nuclei as obtained by the alpha particle method is given in table 18.

Figure 21 shows the prong distribution observed in the present experiment and those observed by Lock and March and Lock et al. using incident protons with an energy of 600 and 950 MeV. The three experiments have been normalised to the same total number of stars.

The number of stars with more than 9 prongs in the present experiment shows that the neutron beam probably contains many neutrons with an energy higher than 600 MeV. If the present results are directly comparable with the proton results the continued rise in the number of stars with decreasing prong number for prong numbers between 6 and 2, an effect not observed in the 950 MeV proton data, might indicate a number of low energy neutrons in the beam.

To take into account the difference in charge of the bombarding particle the number of prongs in a neutron induced reaction should perhaps be modified when compared with proton induced reactions. Cross sections for various processes in p-p and n-p collisions at an energy of the order of 600 MeV, at which the most detailed information is available, are given in table 19. These cross sections were obtained using the results of Prokoshkin and Typakin (1957), Dzhelepov et al. (1956), and others at Dubna. The

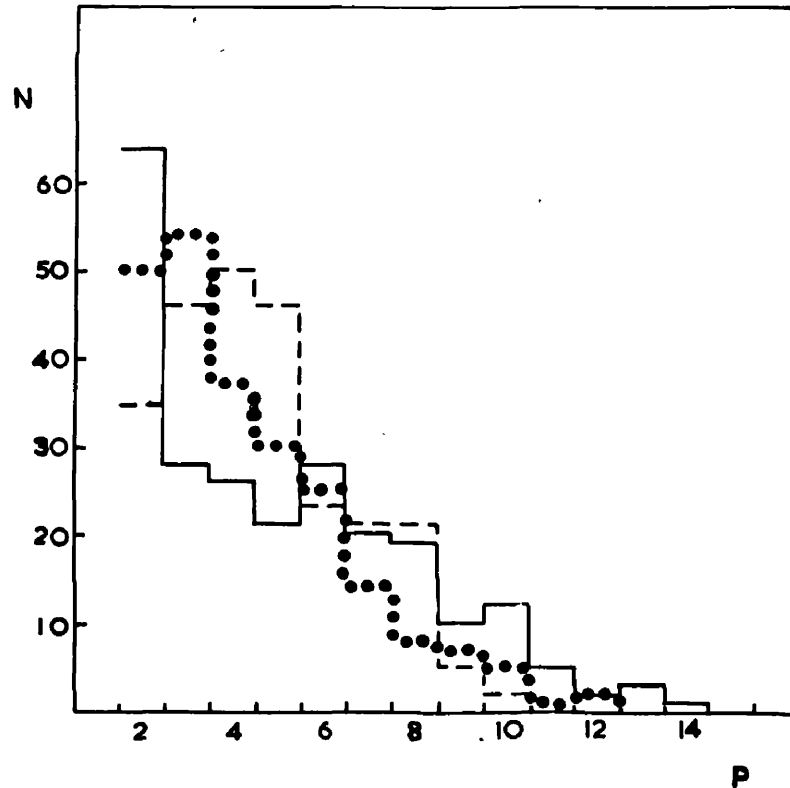


Figure 21 Number of events (N) against number of prongs (P)
Dashed line, results of Lock and March (1955)
Dotted line, present results
Solid line, results of Lock et al. (1955)

number of charged secondaries produced is also shown in table 19. From these results it is found that the total number of charged secondaries in a proton induced reaction divided by the total number of charged secondaries in a neutron induced reaction is 1.6. Hence when comparing stars induced by neutrons with stars induced by protons at high energies the most valid procedure is perhaps to add 0.6 prongs to stars with a small number of prongs and leave unaltered stars with many prongs. This modified prong distribution tends to be flatter than the unmodified results and closer to the 950 MeV proton results.

Table 19

Cross sections at 600 MeV

Reaction	mb	charged secondaries
$p+p \rightarrow p+p$	20	2
$\rightarrow p+p+\pi^0$	3.6	2
$\rightarrow p+n+\pi^+$	14.2	2
$n+p \rightarrow n+p$	20.1	1
$\rightarrow p+p+\pi^-$	3.6	3
$\rightarrow n+n+\pi^+$	3.6	1
$\rightarrow p+n+\pi^0$	7.1	1

The increase in the number of events with high prong number as the bombarding energy increases is

usually explained in terms of both the increase in excitation energy and the absorption of π -mesons produced in the individual nucleon-nucleon collisions taking place within the nuclei. At energies of the order of 2000 MeV (Lanutti et al., loc. cit.) the prong distribution is almost flat for prong numbers less than 11.

The total mean prong number of the unmodified neutron result is 4.4. The total mean prong number as given by Lock et al. for protons with an energy of 950 MeV is 4.26. However, this figure includes one prong events. When these are eliminated the mean prong number becomes 5.0. Hence the difference in mean prong number of the 950 MeV proton experiment and the present experiment is 0.6, in good agreement with the theoretical result deduced above.

(v) Energy Distribution of Prongs

Since most of the prongs left the emulsion before stopping the energy of nearly all prongs was obtained by grain counting. Using the usual notation, first proposed by Brown et al. (1949), tracks were divided into three groups according to their grain density.

Let g^0 be the grain density of a particle at

minimum ionisation. Then particles with a grain density between $1.4g^0$ and g^0 are referred to as 'shower' tracks. For protons $1.4g^0$ corresponds to a kinetic energy of about 450 MeV and for mesons about 60 MeV. Tracks with a grain density between $1.4g^0$ and $6g^0$ are referred to as 'grey' tracks. The upper limit in this case corresponds to a proton with an energy of about 30 MeV. The remaining tracks are referred to as black tracks.

The average number of shower, grey and black tracks per star is given in table 20. Also in this table is given the corresponding distribution for stars induced by 950 MeV protons as reported by Lock et al..

Table 20

Average number of tracks of various energy per star.

	Shower	Grey	Black	Total
Present Results	0.31	1.55	2.54	4.4
950 MeV Protons	0.54	1.11	2.61	4.26

The 950 MeV proton data contains one prong events and so is not directly comparable with the present results. If it is assumed that the secondary of all one prong events is a shower or a grey track the average number

of shower plus grey tracks per star becomes 2.4 and this has to be compared with the value 1.9 obtained here. This again agrees with the theoretical difference derived above. The average number of black tracks observed in the proton and neutron experiments are equal within statistics.

The mean number of grey plus shower tracks as a function of star size is given in table 21 for proton and neutron induced stars.

Table 21

Mean number of grey plus shower tracks.

Prong number	2-4	5-7	8-11
Neutron stars	1.4	2.3	2.8
Proton stars	1.7	2.3	2.3

(vi) Angular Distribution of Prongs

The angular distribution of shower, grey and black tracks is given in figure 22. These results indicate, as expected, that the angular distribution of emitted particles tend to isotropy as the energy of the emitted particle decreases.

The forward to backward ratio of shower, grey and black tracks was 6.5, 3.2 and 1.5 and the results obtained for 950 MeV protons was 22 ± 7 , 5 ± 1.5 and 1.4 ± 0.1 . The

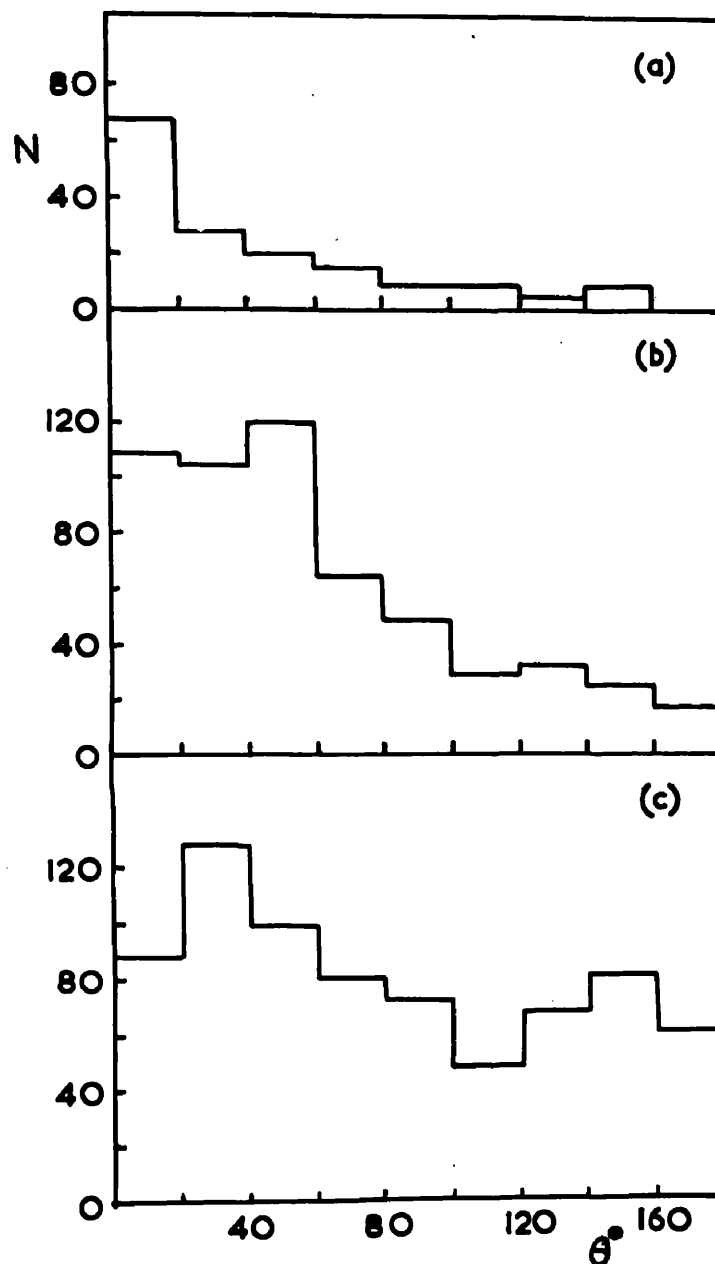


Figure 22 Number of prongs (N , arbitrary units) per unit solid angle against the angle (θ) to the incident neutron direction.

(a) Shower tracks

(b) Grey tracks

(c) Black tracks

only discrepancy between the two sets of results occurs for shower tracks. However, the proton results contain one prong events which were not included in the present investigation. If the same relative number of one prong events are assumed in the present experiment as found by these authors and it is assumed that these are all shower tracks at an angle of 20° to the incident neutron direction then the forward to backward ratio becomes 17 in satisfactory agreement with the results of Lock et al..

B. n-p Interactions

Rosenfeld (1954) showed assuming charge independence that the cross section for meson production in individual nucleon-nucleon collisions could be represented as sums of the three partial cross sections σ_{ii} , σ_{oi} , and σ_{io} where in σ_{ij} the i and j represent isotopic spin states of the initial and final nucleons. Using these results it is possible to interrelate cross sections for the fundamental meson production processes in two nucleon collisions. The cross section for the reaction $n+p \rightarrow p+p+\pi^-$ is given by $\frac{1}{2}(\sigma_{ii} + \sigma_{oi})$

(1) Analysis of Events

A given volume of emulsion was scanned specifically

for three prong events resulting from the collision of a neutron with a hydrogen atom. An analysis of such events is made difficult by the uncertain neutron energy. All events which appeared that they might balance momentum in the up-down and left-right direction were subjected to analysis. Using only the angles at which the tracks were observed with respect to the incident neutron direction and kinematics the ratio of the momentum of each secondary to the momentum of the incident neutron was obtained. Sternheimer (1954) gave the maximum proton angle in the $n+p \rightarrow p+p+\pi^-$ reaction as a function of neutron energy. Applying this condition it was possible in many cases to assign one of the observed tracks to the meson. Multiple meson production at the energy considered here may be neglected. If it was not possible to assign one of the tracks to the meson each track was considered to be the meson in turn. By assuming various values for the incident neutron energy the most suitable value was found to give prongs at the observed angles. In many cases a neutron energy outwith the energy available was required and hence such events were eliminated. The prongs of the remaining events were grain counted and those with an energy determined in this way compatible with the energy

obtained by kinematic considerations were assumed to be true events.

(ii) Cross Section for $n+p \rightarrow p+p+\pi^-$

Four events of the type $n+p \rightarrow p+p+\pi^-$ were found in 430 three prong stars. If it is assumed that the cross section for formation of three prong stars is equal for neutrons and protons then the cross section obtained by 'along the track scanning' by Lock et al. may be used here to obtain the cross section for the reaction studied. These authors obtained the cross section 1300 mb for the interaction of protons with an energy of 950 MeV with the nuclei of nuclear emulsions. Since they found 30 three prong events in a total of 262 events their cross section for three prong events is 149 mb. Hence the cross section for the reaction studied is 1.4 ± 2 mb. If it is assumed that the cross section for a four prong proton induced event is equivalent to a three prong neutron event the corresponding cross section is also 1.4 ± 2 mb.

The results of Hughes et al. (1957) at an energy of 924 MeV on the reaction $p+p \rightarrow p+p+\pi^0$ gives $\sigma_{\pi^0} = 6 \pm 2$ mb and so using this value and the experimental value obtained above for $\frac{1}{2}(\sigma_{\pi^+} + \sigma_{\pi^-})$ the value of σ_{π^+} is obtained as 0 ± 3 mb.

Results of Batson and Riddiford (Private communication by W.O. Lock) on the reactions $n+p \rightarrow p+p+\pi^-$ and $n+p \rightarrow p+n+\pi^0$ using a deuterium filled diffusion cloud chamber, give $\sigma_{0,1} = 0.2 \pm 1.3$ mb and $\sigma_{0,1} = 16 \pm 7$ mb respectively. Hence the present experiment is in agreement with the results obtained in the $n+p \rightarrow p+p+\pi^-$ study.

Future Prospects

In the study of the $n+p \rightarrow p+p+\pi^-$ reaction described above all true events appeared to be initiated by a neutron with an energy of the order of 900 MeV. The study of the interaction of neutrons with complex nuclei also indicated many high energy neutrons in the neutron beam. Hence it appears possible to study the reaction $n+p \rightarrow p+p+\pi^-$ in more detail by obtaining good statistics on energy and angle of emitted particle.

APPENDIX /.

Let the radiating foil be on the X-Z plane and the emulsion surface on the X-Y plane with the scanning region defined by $X=\underline{+F}$ and $Y=H$ to $Y=J$, as shown in figure 23. If $P(x_1, 0, z_1)$ is a fixed point on the foil and PA is the direction of a proton from the foil reaching the emulsion at the point A and making an angle θ with the incident neutron direction PR then the locus of A is given by

$$(x - x_1)^2 + z_1^2 = y^2 \tan^2 \theta$$

which is the equation of a hyperbola. Let the hyperbola cut the lines $X=\underline{+F}$, $Z=0$ at the points S and T. Then three cases arise according as (a) the curve SAT cuts the line $Y=H$, $Z=0$, (b) lies between $Y=H$ and $Y=J$, or (c) cuts the line $Y=J$. The angular limits of θ are easily obtained from equation (A.1) for each of these cases.

Case (b) will be considered.

Let the line PS meet the plane $Y=W$, where W is an arbitrary constant, in V and the line PT meet this plane in Q. Then the points V and Q define an arc of a circle on the plane $Y=W$. The coordinates of V are

$$\left\{ \frac{(y_s - W)(x_1 - x_s)}{y_s} + x_s, W, \frac{z_1}{y_s} (y_s - W) \right\}$$

and a similar result exists for Q. Hence the probability that a proton originating at P and at an angle θ to the

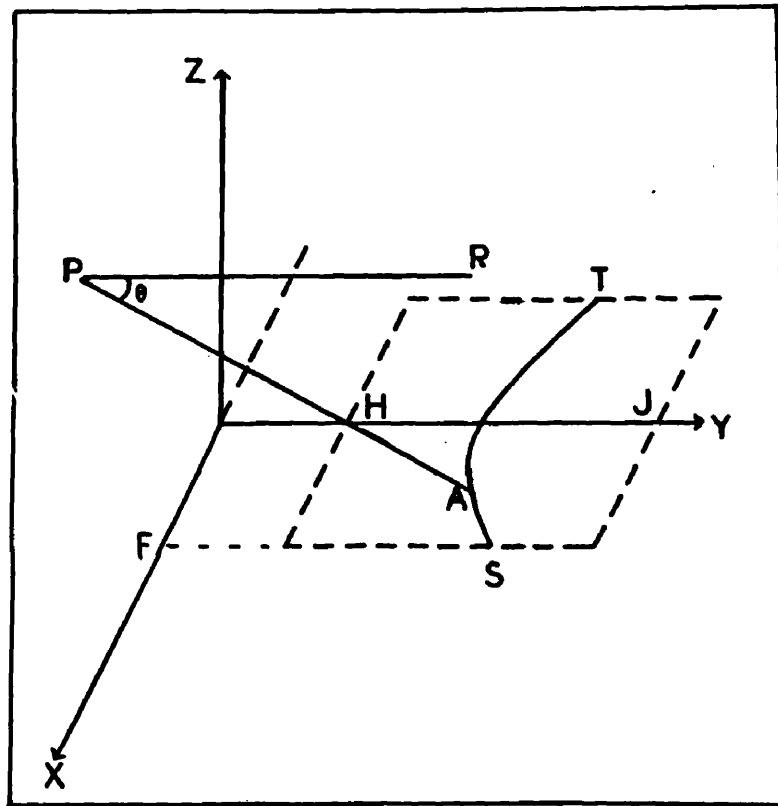


Figure 23 Geometry of aluminium exposure

incident neutron direction will pass through the area scanned is $\frac{1}{\pi} \sin^{-1} \left(\frac{VQ}{2W \tan \theta} \right)$

where $\left(\frac{VQ}{W} \right)^2 = \left\{ x, \left(\frac{1}{y_T} - \frac{1}{y_s} \right) + F \left(\frac{1}{y_T} + \frac{1}{y_s} \right) \right\}^2 + z,^2 \left(\frac{1}{y_T} - \frac{1}{y_s} \right)^2$

A similar formula exists for the other two cases.

72 points equally spaced were picked on the foil and summation carried out over the foil.

PUBLICATIONS

A Study of Protons Emitted from Aluminium, Iron and Rhodium
on Bombardment with Neutrons of 13.2 MeV,

By G. Brown, G.C. Morrison, H. Muirhead and W.T. Morton,
1957, Phil. Mag., 2, 785.

The Protons Emitted from Iron-54 and Iron-56 on Bombardment
with 13.5 MeV Neutrons, By P.V. March and W.T. Morton,

1958, Phil. Mag., 3, 143,

and Proc. Columbia Conf., Sept. 1957, 248.

The Energy and Angular Distributions of the Protons from the
Reaction $\text{Ni}^{60}(\text{n},\text{p})\text{Co}^{60}$ Induced by 13.5 MeV Neutrons,

By P.V. March and W.T. Morton,

1958, Phil. Mag., 3, 577.

Charged Particles Emitted From Aluminium on Bombardment
with 14 MeV Neutrons, By P.V. March and W.T. Morton,

Accepted for Publication in Phil.Mag..

REFERENCES

- ALLAN, D.L., 1957, Proc. Phys. Soc., A, 70, 195.
- ALLAN, D.L., 1958, Nuclear Physics, 6, 464.
- AMALDI, E., BOCCIARELLI, D., CACCIAPUTO, C., and
TRABACCHI, G., 1946, Nuovo Cim., 3, 203.
- ARMSTRONG, A.H., and BROLLEY, J.E., 1955, Phys. Rev., 99, 330.
- AUSTERN, N., BUTLER, S.T., and McMANUS, H., 1953,
Phys. Rev., 92, 351.
- BARSCHALL, H., 1952, Phys. Rev., 86, 231.
- BETHE, H.A., 1940, Phys. Rev., 57, 1125.
- BERNARDINI, G., BOOTH, E.T., and LINDENBAUM, S.J., 1952a,
Phys. Rev., 85, 826.
- BERNARDINI, G., BOOTH, E.T., and LINDENBAUM, S.J., 1952b,
Phys. Rev., 88, 1017.
- BLASER, J.P., BOEHM, F., MARMIER, P., and PEASLEE, D.C.,
1951a, Helv. Phys. Acta, 24, 3.
- BLASER, J.P., BOEHM, F., MARMIER, P., and SCHERRER, P.,
1951b, Helv. Phys. Acta, 24, 441.
- BLATT, J.M., and WEISSKOPF, V.F., 1952, Theoretical Nuclear
Physics (New York: Wiley).
- BLOSSER, H.G., GOODMAN, C.D., HANDLEY, T.H., and RANDOLPH, M.L.
1955, Phys. Rev., 100, 429.

- BUTLER, S.T., 1957, Phys. Rev., 106, 272.
- BOHR, N., 1936, Nature, 137, 344.
- BOOTH, N.E., LEDLEY, B., WALKER, D., and WHITE, D.H., 1957,
Proc. Phys. Soc., A, 70, 209.
- BOOTH, N.E., HUTCHINSON, G.W., and LEDLEY, B., 1958,
Proc. Phys. Soc., 71, 293.
- BROWN, R.H., CAMERINI, U., FOWLER, P.H., HEITLER, H.,
KING, D.T., and POWELL, C.F., 1949, Phil. Mag., 40, 862
- BROWN, G., MORRISON, G.C., MUIRHEAD, H., and MORTON, W.T.,
1957, Phil. Mag., 2, 785.
- BROWN, G., and MUIRHEAD, H., 1957, Phil. Mag., 2, 473.
- CAMERON, A.G.W., 1957, Can. J. of Phys., 35, 666.
- CHEN, F.F., LEAVITT, C.P., and SHAPIRO, A.M., 1955,
Phys. Rev., 99, 857.
- CLEMENTEL, E., and VILLI, C., 1955, Nuovo Cim., 2, 176.
- COHEN, B.L., 1957, Phys. Rev., 105, 1549.
- COHEN, B.L., and NEWMAN, E., 1955, Phys. Rev., 99, 718.
- COLLI, L., and FACCHINI, U., 1956, Nuovo Cim., 4, 671.
- COLLI, L., and FACCHINI, U., 1957, Nuovo Cim., 5, 309.
- COLLI, L., FACCHINI, U., IORI, I., MARCAZZAN, G., SONA, A.,
PIGNALLI, M., 1958, Nuovo Cim., 7, 400.
- COOK, L.J., McMILLAN, E.M., PETERSON, J.M., and SEWELL, D.C.,
1949, Phys. Rev., 75, 7.

COOR, T., HILL, D.A., HORNYAK, W.F., SMITH, L.W., and

SNOW, G., 1955, Phys. Rev., 98, 1369.

CRANBERG, L., and LEVIN, J.S., 1956, Phys. Rev., 103, 343.

CULLER, G., FERNBACH, S., and SHERMAN, N., 1956,

Phys. Rev., 101, 1047.

DAINTON, A.D., GATTIKER, A.R., LOCK, W.C., 1951, Phil. Mag.,

42, 396.

DZANTIEV, B.G., LEVKOVSKII, V.N., MALIERSKII, A.D., 1957,

Dokl. Akad. Nauk. S.S.R., 113, 537.

DZHELEPOV, V.P., KAZARINOV, Yu.M., GOLOVIN, B.M., FLJAGIN, V.I.

and SATAROV, V.I., 1956, Nuovo Cim., 3, Supp. 1., 61.

EASTMAN, P.C., ISENER, N.R., BAINBRIDGE, G.R., and

DUCKWORTH, H.E., 1956, Phys. Rev., 103, 145.

EISBERG, R.M., and IGO, G., 1954, Phys. Rev., 93, 1039.

ELTON, L.R.B., and GOMES, L.C., 1957, Phys. Rev., 105, 1027.

ENDT, P.M., and KLUYVER, J.C., 1954, Rev. Mod. Phys., 26, 95.

FEATHER, N., 1953, Adv. in Phys., 2, 141.

FERMI, E., and AMALDI, E., 1935, Ric. Sci., A6, 544.

FERNBACH, S., SERBER, R., and TAYLOR, T.B., 1949,

Phys. Rev., 75, 1352.

FERNBACH, S., and WEISSKOPF, V.F., 1949, Phys. Rev., 76, 1550.

FESHBACH, H., PORTER, C.E., and WEISSKOPF, V.F., 1954,

Phys. Rev., 96, 448.

FORBES, S.G., 1952, Phys. Rev., 88, 1309.

- FORD, K.W., and BOHM, D.,1950, Phys. Rev., 75, 718.
- FOWLER, J.L., and BROLLEY, J.E.,1956, Rev. Mod. Phys.,28,103.
- FRANCIS, N.C., and WATSON, K.M.,1953, Amer. J. Phys.,21, 659.
- GOLDBERGER, M.L.,1948, Phys. Rev., 74, 1269.
- ^H
GOSHAL, S.N.,1950, Phys. Rev., 80, 939.
- GRAVES, E.R., and ROSEN, L.,1953, Phys. Rev., 89, 343.
- GUGELOT, P.C.,1951, Phys. Rev., 81, 51.
- GUGELOT, P.C.,1954, Phys. Rev., 93, 425.
- HADLEY, J., and YORK, H.,1950, Phys. Rev., 80, 345.
- HALING, R.K., PECK, R.A., and EUBANK, H.P.,1957, Phys. Rev.,
106, 971.
- HEIDMANN, J., and LEPRINCE-RINGUET, L.,1948, Compt. Rend.,
226, 1716.
- HINDS, S., MIDDLETON, R., and PARRY, G.,1958, Proc. Phys.Soc.,
71, 49.
- HUGHES, I.S., MARCH, P.V., MUIRHEAD, H., and LOCK, W.O.,1957,
Phil. Mag.,2, 215.
- JOHN, W.,1956, Phys. Rev., 103, 704.
- KAPUR, P.L., and PEIERLS, R.,1938, Proc. Roy. Soc.,166, 277.
- KELLY, E.L.,1950, U.C.R.L.,1044.
- LANE, A.M., and WANDEL, C.F.,1955, Phys. Rev.,98, 1524.
- LANG, J.M.B., and Le COUTEUR, K.J.,1954, Proc. Phys. Soc.,
A, 67, 856.

- LANUTTE, J., GOLDHABER, G., and GOLDSACK, S.J., 1955, Bull. Am. Phys. Soc., 30, 3, E.1. and Private communication.
- LEES, C.F., MORRISON, G.C., MUIRHEAD, H., and ROSSER, W.G.V., 1953, Phil. Mag., 44, 304.
- LOCK, W.O., and MARCH, P.V., 1955, Proc. Roy. Soc., A, 230, 222.
- LOCK, W.O., MARCH, P.V., MUIRHEAD, H., and ROSSER, W.G.V., 1955a, Proc. Roy. Soc., A, 230, 215.
- LOCK, W.O., MARCH, P.V., and McKEAGUE, R., 1955b, Proc. Roy. Soc., A, 231, 368.
- MILLER, D.W., ADAIR, R.K., BOCKELMAN, C.K., and DARDEN, S.E., 1952, Phys. Rev., 88, 83.
- MOON, P.B., and TILLMAN, J.R., 1935, Nature, 135, 904.
- MORRISON, G.C., MUIRHEAD, H., and MURDOCH, P.A.B., 1955, Phil. Mag., 46, 795.
- MORRISON, G.C., MUIRHEAD, H., and ROSSER, W.G.V., 1953, Phil. Mag., 44, 1326.
- MOSKALEV, V.I., and GAVRILOVSKII, B.V., 1956, Dokl. Akad. Nauk. S.S.R., 110, 972.
- NEWTON, T.D., 1956, Can. J. Phys., 34, 804.
- PAUL, E.B., and CLARKE, R.L., 1953, Can. J. Phys., 31, 267.
- PEASLEE, D.C., 1955, Ann. Rev. of Nucl. Sci., 5, 99.
- PHILBERT, G., 1956, Comp. Rend. Acad. Sci., 234, 141.
- PROKOSHKIN, Yu, D., and TYPAKIN, A.A., 1957, J.E.T.P., 32, 750.

- RIBE, F.L., and DAVIS, R.W., 1955, Phys. Rev., 99, 331.
- ROSENFELD, A.H., 1954, Phys. Rev., 96, 139.
- ROTBLAT, J., 1951, Nature, 167, 550.
- SERBER, R., 1947, Phys. Rev., 72, 1114.
- SHAPIRO, M.M., 1953, Phys. Rev., 90, 171.
- SHOUPP, W.E., JENNINGS, B., and SUN, K.H., 1949, Phys. Rev., 75, 1.
- STEBLER, A., and HUBER, P., 1948, Helv. Phys. Acta, 21, 59.
- STERNHEIMER, R.M., 1954, Phys. Rev., 93, 642.
- WAFFLER, H., 1950, Helv. Phys. Acta, 23, 239.
- WALKER, R.L., 1949, Phys. Rev., 76, 244.
- WALT, M., BECKER, R.L., OKAZAKI, A., and FIELDS, R.E., 1953, Phys. Rev., 89, 1271.
- WEISSKOPF, V.F., 1937, Phys. Rev., 52, 295.
- WEISSKOPF, V.F., 1957, Nuclear Physics, 3, 423.
- WEISSKOPF, V.F., and EWING, D.H., 1940, Phys. Rev., 57, 472.
- WHITMORE, B.G., and DENNIS, G.E., 1951, Phys. Rev., 84, 296.
- WIGNER, E.P., and EISENBUD, L., 1947, Phys. Rev., 72, 29.
- WOLFENSTEIN, L., 1951, Phys. Rev., 82, 690.
- WOODS, R.D., and SAXON, D.S., 1954, Phys. Rev., 95, 577.

ACKNOWLEDGEMENTS

I would like to thank Dr. A. M. Ward for help during the exposures at the Glasgow H.T. set and Mr. B. A. Munir for carrying out the exposures at the Birmingham synchrotron. I would also like to express my gratitude to Dr. H. Muirhead and Dr. P. V. March for their help in all possible ways and to Professor P. I. Dee F.R.S. for his interest and encouragement.